Superparamagnetic Nanoparticles for Magnetic Resonance Imaging (MRI) Diagnosis

by

Yunyu SHI

School of Chemical Engineering
The University of Adelaide

A thesis submitted for the degree of Master of Engineering Science

The present work contains no material which has been accepted for the award of any other degree or diploma in any university or other tertiary institution and, to the best of my knowledge and belief, contains no material previously published or written by another person, except where due reference has been made in the text.

I give consent to this copy of my thesis, when deposited in the University Library, being available for loan and photocopying.

Signed:

Date:

ABSTRACT

The main strategy for treating solid cancers is based on the very early diagnosis of a malignant tumor, and in general the smaller the tumor, the greater the likelihood of successful treatment. Magnetic Resonance Imaging (MRI), based on the nuclear magnetic resonance phenomenon, provides the possibility of detecting early malignant tumors with the assistance of appropriate contrast agents. Hence, researchers continue to develop novel magnetic materials to achieve this aim. Superparamagnetic nanoparticles have become the focus of these studies because their superparamagnetic, biocompatible and hydrophilic properties would be revealed after modifying the particle surface by suitable surfactants. Considerable research in this area has provided valuable insights; however, suitable magnetic materials that can fulfill all the requirements of MRI application are still under investigation.

Surface modification of superparamagnetic nanoparticles towards their use as MRI contrast agents has been the topic for many researchers, but implementation into fully functional *in vivo* procedures still remains as a challenging task. In the present study, high quality monocrystalline iron oxide nanoparticles have been synthesised and surface-modified with carboxymethylated dextran as well as polyethylene glycol (PEG). Dextran and PEG macromolecules with low and high carboxyl contents were synthesized and grafted onto dopamine-iron oxide nanoparticles. Furthermore, the coating procedure was optimised to prevent aggregation among the nanoparticles. Dextran-coated and PEG-coated nanostructures were characterised by using X-ray Photoelectron Spectroscopy (XPS), Fourier Transformer Infrared Spectroscopy (FTIR), Transmission Electron Microscopy (TEM) and Dynamic Light Scattering (DLS). Consequently, mono-dispersed dextran coated nanoparticles were obtained with an approximate hydrodynamic diameter of 50 nm. The resulting coated nanoparticles exhibited the nanostructures with an excellent colloidal stability in physiological environment even at high salt concentration. The resistance to non-specific protein adsorption was investigated in an *in vitro* model. Both dextran-coated and PEG-coated nanoparticles displayed low non-specific adsorption. However, the free carboxyl groups could be activated to covalently immobilize proteins.

ACKNOWLEDGMENTS

Many individuals and several organizations have contributed to this project. Firstly, I want to acknowledge my supervisors: Dr. Yung Ngothai (The University of Adelaide), Prof. Peter Majewski (Ian Wark Research Institute, University of South Australia), Dr. Benjamin Thierry (Ian Wark Research Institute, University of South Australia) and Associate Prof. Dzuy Q. Nguyen (The University of Adelaide) for their helpful guidance and kind encouragement. Their significant efforts in my masters program were extraordinarily helpful and highly appreciated. I am also grateful to the staff and my colleagues in the School of Chemical Engineering, The University of Adelaide as well as those in Ian Wark Research Institute (IWRI). Their friendship, assistance and encouragement lightened the heavy load of postgraduate study.

This research project has been conducted mostly at IWRI of UNISA. Especially, I wish to thank Dr. Benjamin Thierry and Prof. Peter Majewski who have initiated the project, supervised me and provided experimental facilities, chemicals and technical guidance on superparamagnetic nanoparticles and their bio-applications.

Also, I wish to thank Dr. Karen Adams and the other teachers from Integrated Bridging Program (IBP) who helped and guided me to start up my research project when I first arrived as an overseas student.

Last but not least, I am grateful to my parents for their financial support during my postgraduate studies and my wife, Yan Chen, for her love and constant support.

PUBLICATIONS

Y. Shi, P. Majewski, Y. Ngothai, D. Q. Nguyen and B. Thierry, in press, High Quality Mono-disperse Dextran-Coated Magnetic Nanoparticles for Magnetic Resonance Imaging, CHEMECA 2006, Auckland.

TABLE OF CONTENT

LIST OF FIGURES

1 INTRODUCTION

The current study integrates body science, chemical engineering and nano-technology, which are the core areas that actively aim to promote the quality of human life. Since the 1990s, there has been an increasing research interest into nano-technology, which focuses on nano-sized particles, the dimensions of which are in the range of 1 nanometer to several hundred nanometers diameter of material (Horn et al., 2001). Over several decades, researchers have learned that, due to the extremely high ratio of surface area to volume of the nano-scaled materials, these materials display dramatically different physical and chemical properties, such as higher adsorption capability of solid nano-powder and different magnetic performance of magnetic materials, to the millimeter or micrometer sized materials. Therefore, nano-scaled materials have potential for applications in various fields of industry and science, including waste treatment, energy and medicine.

The concept of the superparamagnetism of magnetic materials in the nano-scale was speculated by Frenkel and Dorfman in 1930. Subsequent studies demonstrated the accuracy of this speculation. That is if the nanoparticles were produced from magnetic materials and the particle size was small enough, these nanoparticles would display superparamagnetic properties. In addition, when these superparamagnetic nanoparticles were coated by an appropriate layer, they could disperse into a water-based solution and remain stable in the solution, thus forming ferrofluid. These ferrofluid can be used in various bio-applications, including *in vivo* and *in vitro* applications. Several previous studies have investigated this novel research area (Olsvik et al., 1994; Schutt et al., 1997; Schutt et al., 1999; Burke et al., 2001; Puntes et al., 2001; Bharali et al., 2003; Gee et al., 2003; Harisinghani et al., 2003; Harris et al., 2003; Gupta et al., 2004; Neuberger et al., 2005), but have been unable to overcome several disadvantages, as discussed later in this thesis.

Bio-applications of superparamagnetic nanoparticles include *in vitro* applications

(Prestvik et al., 1996), like cell, antibody or many other bio-unit separations, and *in vivo* applications, such as drug delivery (Alexiou et al., 2000; Torchilin, 2000), hyperthermia procedures (Jordan et al., 1999; Ito et al., 2004; Ivkov et al., 2005) and MRI contrast agents (Schutt et al., 1999; Portet et al., 2001; Harisinghani et al., 2003; Jun et al., 2005; Neuberger et al., 2005; Song et al., 2005; Tartaj et al., 2005). In order to use the magnetic materials *in vitro* or *in vivo*, size distribution, biocompatibility, toxicity, surface chemical properties and various other parameters should be considered in advance. Especially for *in vivo* applications, the opsonization (i.e. a process where molecule acts as binding enhancer) and phagocytosis (i.e. cell eating) by the reticulendothelial system (RES) are the barriers to the uptake of magnetic nanoparticles and their retention in circulation for the desired period of time (Neuberger et al., 2005; Owens III et al., 2005). Thus, surface modification with functional groups could be one of the strategies for solving this problem.

The aims of this project were to develop two types of water-based ferrofluids for MRI diagnosis. It also aimed to determine the optimum method to generate Fe-based nanoparticles in mixture solution of hydrophilic surfactants and pure water. In current study, the biocompatible surfactants such as dextran and polyethylene glycol (PEG), were induced to form a coating on the surface of the nanoparticles. The hydrophilic chemical coating of the nanoparticles produced a stable dispersion in the aqueous solution and prevented the particles from opsonization and phagocytosis by RES. Hence the coating could provide a chemically controllable surface which could be used to localise the therapeutic sites.

2 LITERATURE REVIEW

This chapter reviews literature and describes in detail the background information of the project, identifies the problems of previous studies, and, in the later section, proposes the research process for the present study.

2.1 Superparamagnetism

Over 75 years ago, Frenkel and Dorfman (1930) speculated on the possible behaviour of ferromagnetic nano scale particles, and their speculation has been demonstrated to be correct in later studies. The magnetic properties of the ferromagnetic particles are changed dramatically by quantum size effects and increased surface area of the nano-scaled magnetic particles. Bulky sized particles of magnetic materials display ferromagnetic properties due to their multi-domain structure of the particles. These magnetic domains interact with each other and spin in a single particle coupled together. Such materials are said to be ferromagnetic because they have magnetic properties regardless of the existing of an applied magnetic field. A particle of the magnetic material below a critical diameter, depending on the particle material, approximately 8 nm for •-Fe_2O_3 particles (Schmidt, 2001), contains only one single magnetic domain, so that this particle is at a state of uniform magnetization at any field without interaction with neighbour domains in one particle or a well dispersed suspension. In fact, the critical diameter is the single domain size of the materials. Hence, an object consisting of many of these nano-sized particles displays magnetic properties under an applied magnetic field, but permanent magnetization would not remain when the applied magnetic field has been removed (Harris et al., 2003). The reason for this phenomenon, superparamagnetism, is that these domains will return to disordered status by having enough space to refuse the interaction between each other while there is no extra magnetic field applied.

This specific characteristic make superparamagnetic nanoparticles a valuable

research subject for considerable bio-applications (Olsvik et al., 1994; Meza, 1996), and, many potential applications have been investigated and developed by researchers in the last decades (Olsvik et al., 1994; Schutt et al., 1997; Schutt et al., 1999; Torchilin, 2000; Neuberger et al., 2005).

2.2 Bio-applications of Superparamagnetic Nanoparticles

The biomedical applications of the superparamagnetic nanoparticles could be categorised into *in vitro* applications and *in vivo* applications, and a dramatic increase in the number of these applications has appeared in the past several years (Neuberger et al., 2005).

In *in vitro* studies, immune magnetic separation techniques of cells, proteins, DNA/RNA, bacteria, viruses and other biomolecules have been investigated extensively (Olsvik et al., 1994; Prestvik et al., 1996; Neuberger et al., 2005). Studies on these areas have already achieved enormous success. Furthermore, the *in vivo* applications of superparamagnetic nano-structured materials have also been studied by many researchers (Poste et al., 1984; Meza, 1996; Jordan et al., 1999; Schutt et al., 1999; Bordat et al., 2000), and some of the *in vivo* applications are more directly related to our daily life than those for research purposes, such as the clinical studies of cancer therapy and diagnosis of early cancer cells. Three typical applications in this specific area are drug targeting and delivery (Oppenheim, 1981; Kreuter, 1983; Torchilin, 2000), magnetic fluid hyperthermia procedure (Jordan et al., 1999; Gangopadhyay et al., 2005; Gonzales et al., 2005) and contrast agents of MRI diagnosis (Chambon et al., 1993; Chouly et al., 1996; Portet et al., 2001).

2.2.1 Drug Delivery

For pharmacotherapy of malignant tumours, one of the biggest challenges is to accurately deliver the appropriate amount of drug to a desired location inside the body and to maintain the dose for an adequate duration (Neuberger et al., 2005). Accurate drug delivery could avoid high concentration intake of drug by patients, and thus decreasing the possibilities of side effects (Lubbe et al., 1996; Lubbe et al., 1996; Alexiou et al., 2000). Using superparamagnetic nanoparticles as the carrier provides a physical and chemical targeting method for drug delivery. Drugs bound in this way could be delivered with ease to the diseased location by use of an external magnetic field (Lubbe et al., 1999; Neuberger et al., 2005). In

addition, functionalized particle surface could selectively attach to specific cells to deliver and localize bound drug (Poste et al., 1984; Torchilin, 2000).

Therefore, by using superparamagnetic nanoparticles as carrier, drug delivery can be affected by various characteristics of the drug bound particles. As well as physical properties, concentration of the suspension of the particles and the inject dosage of the suspension, the drug binding type with the magnetic particles also affects the efficiency of drug delivery (Lubbe et al., 1999; Neuberger et al., 2005). Moreover, the particle size distribution, immobilized functional group on particle surface, intensity of applied magnetic field and the particle injection route, as well as some physiological conditions of the patients may affect drug delivery procedure. However, from the chemical engineering viewpoint, the superparamagnetic nanoparticles already have significant potential capability for drug delivery application.

2.2.2 Hyperthermia Procedure

Chemotherapeutics, as an important therapeutics for cancer patients, has extremely strong damage to other normal organs of the patients at the same time that the cancer cells were being killed. Therapeutic temperature beyond 56 ^{o}C causes necrosis, coagulation and carbonization of the normal tissues of patients during chemotherapeutic procedure (Jordan et al., 1999; Neuberger et al., 2005). Thus, conventional hyperthermia treatments have obvious disadvantages on selectivity of therapeutic sites. This reason is preventing the clinical application of chemotherapeutics.

However, hyperthermia procedure with magnetic ferrofluid offers possibility of specific localized heat induction. The superparamagnetic nanoparticles could induce extra heat to local area through the oscillation of the magnetic moment inside the nanoparticles. As the similar theory to the other applications of magnetic nanoparticles, once the particles target the diseased tissues with help of applied magnetic field or via immobilized specific targeting functional groups (Jordan et al., 1999), nanoparticles have much higher specific adsorption rate than bulky magnetic particles. Hence, cells of solid cancer will be killed while

maintaining normal tissue cells at a lower temperature below 41~46 ºC (Gonzales et al., 2005). Due to the superior property of these magnetic nanoparticles have, hyperthermotherapeutics increase the efficiency of the treatment of solid cancer..

2.2.3 Contrast Agents for Magnetic Resonance Imaging (MRI)

MRI is a common tool for diagnosis of malignant tumors. This technique is based on nuclear magnetic resonance phenomenon. This phenomenon occurs because the nucleus of different atoms absorbs different strengths of energy and resonates at a certain resonance frequency when the applied magnetic field is periodically changed. Hydrogen is one of the most appropriate elements for nuclear magnetic resonance effect, and, is the most common element contained in human body. For this reason, MRI can provide clear images of anatomical detail and soft tissue. The first human body imaging was performed in 1977. Moreover, compared to X-ray scan and Computerized Tomography (CT), MRI provides more legible images of both bones and soft tissues of the human body, and is a safer method for detection (Feeney, 1996), because bone structures absorb the X-ray and block the penetration of the X-Ray during CT scanning. Another advantage of MRI is its safety and ability to scan without radiation so that it does not destroy healthy cells in the human body. MRI became more useful for malignant tumor detection when assisted by contrast agents. The most current common contrast agent contains gelable gadolinium (Gd) cations, which provide a sufficient magnetic moment. In many cases, MRI can provide images more clearly after the intravenous injection of contrast agents. Therefore, MRI is wildly applied to scan of many vital organs including the heart and brain (Frahm et al., 2003; Harisinghani et al., 2003; Nitin et al., 2004; Lee et al., 2005). However, MRI or MRI with contrast conventional agents lacks sensitivity for scanning the very small tumors or even specific solid cancer cells inside the human body because of the weakness of therapeutic site targeting capability. Many researchers have focused on developing new contrast agents for MRI diagnosis in order to enhance the contrast of MRI imaging.

Superparamagnetic nano-structured materials were developed as the contrast

agents for MRI because the nano-scaled structure modified the relaxation time of protons, and enhanced the sensitivity of diagnosis of MRI. In addition, appropriate surface modification of the nanoparticles with suitable biologically active specific functional groups, such as monoclonal antibodies or proteins, increases the specificity of the MRI diagnosis as well. In fact, the first patent of dextran coated iron oxide nanoparticle as contrast agent was registered about ten years ago (Hasegawa et al., 1998). Via intravenous injection of the contrast agents, superparamagnetic nanoparticles are injected into a blood vessel and taken up by the solid cancer cells during circulation. This leads to clear images of soft tissue with magnetic agents.

The quality of the particles used as MRI contrast agent is determined by particle magnetic properties of core material, particle size distribution, particle surface charge, stability in near neutral aqueous solvent or physiological brine and chemical properties of immobilized functional molecules on surface.

2.2.4 Reticulendothelial System (RES)

Opsonization and phagocytosis by the reticulendothelial system (RES) prevent human or animal bodies from intruded foreign substances. The opsonization process will recognize unfamiliar substances as intruders and therefore cover them with opsonin proteins, which could visualise these intruders to phagocytic cells, and hence the recognized foreign substances will be rapidly eliminated from the circulation of the blood and mostly accumulated in the liver and spleen (Illum et al., 1987; Gref et al., 1995; Panagi et al., 2001; Owens III et al., 2005). These processes efficiently remove many harmful and toxic substances to help human or animal recovered from some diseases, but on the other side, they also unselectively arrest the druggery helping cure diseases.

With the presence of nanoparticles in blood circulation regardless the particles are magnetic or non-magnetic, some researchers have found that phagocytosis, biodistribution and pharmacokinetics were closely depended on the particle size and surface coating (Moghimi et al., 1993; Owens III et al., 2005). While the particles coated by a non-biodegradable polymer of molecular weight is under

5,000 or the molecular weight as high as 100,000 for more dense polymer are removed by renal system, most of other particles, especially those larger than 200 nm and the uncoated particles, are sequestered and stored in one of the monoclear phagocytic system (MPS) organs, liver or spleen. In addition, the foreign particles larger than 200 nm and uncoated particles will be removed by RES or renal system extremely quick or even in few seconds after injection (Chouly et al., 1996; Muller et al., 1996; Neuberger et al., 2005).

Nanoparticles applied *in vivo* must prolong the circulation time in blood vessel to reach the therapeutic sites and exert the influence, which means that these particles have to overcome rapid elimination by RES. Based on previous studies, size distribution of the particles and the surface chemical properties play the major roles at this stage. Much longer blood circulation time has been measured with the particles size below 200 nm and with biocompatible polymer coating, typically, such as PEG, dextran (Bautista et al., 2005; Hong et al., 2005). These polymer coatings could efficiently resist the adsorption of the non-specific protein, so that the phagocytic cells cannot recognize the particles as foreign substances very soon. The surface modification on particles is discussed further in later section.

2.2.5 Targeting of Therapeutic Sites

The three typical *in vivo* applications all require that magnetic nanoparticles should accurately localise to therapeutic sites. All the targeting methods could be classified to passive, active and physical targeting (Torchilin, 2000). The physical targeting is localization of the magnetic particles with external assistance, typically by applied magnetic field. However, with the assistance only from outside of the body, the physical targeting has less capability to recognize specific cells or tissues. The passive targeting is contributed by the properties of drug and carrier and, also, the difference between therapeutic sites and other sites. Only the disrupted endothelial lining of tumour tissues allows the drug carrier of smaller size to pass through (Figure 2-1), so that drug carried nanoparticles could be localised by enhanced penetration and retention (EPR) effect (Torchilin, 2000). In active targeting, the specific targeting functional

groups, such as monoclonal antibodies, are immobilized on the particle surface to efficiently increase the chance of uptake by specific cells. Compared to the passive targeting, the active targeting is working with more controllable particles. Thus, the active targeting is more challenging for researchers.

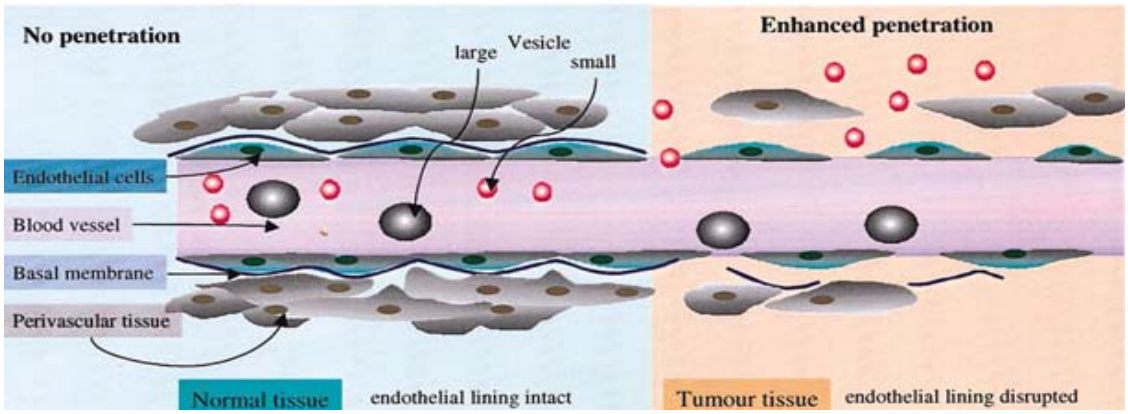

Figure 2-1: Sketch of the process of the passive targeting by “EPR” effect

2.3 Particle Characteristics for *in vivo* Bio-applications

As a product for *in vivo* applications, such as drug delivery, hyperthermia treatment and MRI contrast agent, the superparamagnetic nanoparticles have to stay *in vivo* as long as they were designed with nil or minimal side effect. Nanoparticles for biomedical applications have to fulfil the requirements of applied environment, especially for *in vivo* applications, the conditions are more critical than others. Not only the facts like material and size should be considered, but also many other physical properties of the particles and chemical properties of the modified particle surface, such as biocompatibility and cytotoxicity, should be involved in consideration.

2.3.1 Size Distribution

Size distribution is the first parameter describing the quality when superparamagnetic nanoparticles are being investigated. A size distribution of only a few nano metres has been developed by many researchers with various synthesis procedures (Bee et al., 1995; Gupta et al., 2004; Pinna et al., 2005). However, the dynamic diameter of the nanoparticles in hydrophilic ferrofluid after surface coating plays the vital role at *in vivo* application.

Firstly, only monocrystalline particles or minimal aggregated particles in dispersion would display superparamagnetism and stabilized in suspension with suitable surfactant coating. Whereas particles larger than 400 nm (i.e. the minimal diameter of the capillaries), will be filtered by the lung (Neuberger et al., 2005). In addition, it has been reported that particles which exceed than 200 nm, tend to eliminate immediately by one of the organs from MPS regardless of being polymer coated or not. Moreover, even the particles under 100 nm would be captured mostly by liver in order of from bigger size particles to smaller size particles. So, the phagocytotic activity is size dependent. The smaller the particles, the longer their circulation time in blood vessel. Also, for EPR effect, 10 nm is the penetration threshold of the endothelium, where the limitation could increase to 700 nm when inflammation or tumour infiltration occurred (Schutt et al., 1997; Neuberger et al., 2005).

2.3.2 Cytotoxicity

Cytotoxicity is a vital factor that needs to be considered for *in vivo* application of superparamagnetic nanoparticles. This is because these particles would be captured and stored by some of the organs from MPS after application despite if these particles were coated with biodegradable/non-biodegradable biocompatible surfactants (Neuberger et al., 2005). Acute side effect should be avoided by testing the cytotoxicity of the applied product *in vitro* before injection. Several in vivo tests (Weissleder et al., 1989; Lacava et al., 1999[1,2]) on animals have shown that, with a large dosage of 3,000 µmol Fe of the iron based nanoparticles per kg body weight, the histology and serologic blood tests have indicated that no side effects occurred after 7 days treatment. In view of the *in vivo* environment, the suspension of superparamagnetic nanoparticles requires hydrophilic chemicals as solvent, such as MilliQ water or physiological brine, and be controlled at near neutral where pH value is about 7.4 (Schutt et al., 1997). However, cytotoxicity of every novel product for *in vivo* applications should be examined carefully.

2.3.3 Surface Charge and Protein Adsorption

As bare nanoparticles are unsuitable for in vivo applications, then surface charge and protein adsorption capability are more related to the surfactants bond to the particle surface.

In general, particles with the same electronic charged surface are more stable in dispersion due to the homo-charged surface. The higher the zeta potential, the electrical potential at the shear plane of the double layer, the more stable the dispersion (Neuberger et al., 2005). However, *in vivo* phagocytosis would become more activated with the high charged surface of the nanoparticles (Muller et al., 1996). On the other hand, as the cell membrane is negatively charged, the negatively charged particles would not be attacked by endocytic cells with ease. In conclusion, particles are better to be slightly negatively charged on surface, which is leading up to an agreement with the condition discussed in last section that the pH value of the dispersion should be about 7.4.

Protein adsorption is the first step of opsonization. In fact, prolonging the circulation time in blood vessels is examining the capability of protein adsorption of the coating. Resistance to the non-specific protein adsorption could prevent magnetic nanoparticles from attachment of opsonin proteins and recognization by phagocytic cells in a certain time (Owens III et al., 2005). As for the active targeting purpose, specific protein adsorption needed to be allowed on the particle surface for functionalization of the particles (Torchilin, 2000). With the two requirements mentioned above, protein adsorption capability of the particles need to be under control that is not only resisting to the non-specific protein adsorption, but also adsorbing the specific functional proteins for targeting.

2.4 Preparation of Particles

It is a great challenge to produce magnetic nanoparticles that fulfill all the requirements for a particular application. Existing methods are primarily physical methods and chemical methods. Comparatively, chemical methods, especially the wet chemical methods, are much simpler and more efficient. The most remarkable advantage is that the wet chemical methods have appreciable control of particle size, composition and even the particle shape (Gupta et al., 2004). However, various synthesis procedures were developed by many researchers , and some of these procedures are providing rather high quality of superparamagnetic nanoparticles (Burke et al., 2001; Puntes et al., 2001; Gee et al., 2003; Liz-Marzan, 2004; Gupta et al., 2004).

One of the most popular procedures of iron oxide nanoparticle synthesis, co-precipitation technique, has been widely used for magnetic nanoparticle preparation in studies during last few years. Gupta et al. (2004) described a synthesis procedure of Superparamagnetic Iron Oxide Nanoparticles (SPION). This route directly generates hydrophilic dispersion of iron oxide nanoparticles, which has narrow size distribution of the range from 10 nm to 30 nm, and the particles are mono-dispersed in suspension, in the aqueous solvent. Appropriate surface chemistry could be used to coat over the nanoparticles once the precipitation was formed, so that these nanoparticles were prevented from oxidation. In addition, passing bubbling nitrogen (N_2) gas through the solution during process could control the reaction kinetics in order to reduce the particle size. As Gupta reported, coated by different functional surfactants, SPION has very potential for various applications including MRI contrast agent.

Puntes et al. (2001) presented two possible methods for preparation of Co-based nanoparticles. These are a solution-phase metal salt reduction and a metal carbonyl pyrolysis. The latter method is not very appropriate in the current study because it produces large size particles that do not have superparamagnetic properties. Through injecting an organometallic precursor into a hot surfactant mixture under Ar atmosphere, the shape of the nanoparticles can be controlled. Another way to control the shape of the

nanoparticles is to control the growth rates on different directions of the particles. The surfactant mixture of trioctylphosphine (TOPO) and oleic acid was used to decrease the particle growth rate and control the particle size. However, polymer coating was not presented as main point in this paper.

Burke et al. (Burke et al., 2001) investigated the preparation and characterization of iron-cored nanoparticles with polystyrene (PS) coating, which were prepared by thermal decomposition of iron pentacarbonyl ($Fe(CO)_5$) in the presence of polystyrene-tetraethylene-pentamine (PS-TEPA). This process used 1-methylnaphthalene as the solvent and a single heating cycle which is 95 ºC for 8 hours then 190 ºC for 2 hours. The final product of this procedure contained both simple core-shell particles and larger complex particles, with both particles tightly coated by 2-3 nm of polymer shell and the whole particle diameter is from 10 nm to near 100 nm. The similar technique has been used by Hyeon et al. (Hyeon et al., 2001) with $Fe(CO)_5$ to formed a mono-dispersion of maghemite nanoparticles with a size distribution of approximate 13 nm. In addition, this study was continued by Gao et al. (Gao, 2003). In Gao's study, 13 nm particles were transferred to hydrophilic solvent via ligand exchange in order to prevent from the phagocytosis by RES for *in vivo* applications. More recently, synthesis of mono-dispersion of MFe_2O_4 nanoparticles was reported by Sun et al. (2004). The ferrite nanoparticle suspension was generated by the thermal de-composition of iron acetylacetonate, cobalt acetylacetonate and manganese acetylacetonate. The ferrite nanoparticles could be transferred to hydrophilic solvent after synthesis via ligand exchange.

These studies mentioned above accumulated experience and plenty of understanding on synthesis procedure of superparamagnetic nanoparticles for bio-applications. The co-precipitation technique has already become the common technique employed in synthesis of most of the commercial available magnetite nanoparticles. The high-temperature de-composition technique, which is used to generate the particles under non-aqueous circumstance, so called non-aqueous route as well, overcomes many of the drawbacks of the aqueous precipitation technique as well as other organic synthetic routes (Jun et al., 2005; Pinna et al., 2005; Sun, 2006). Therefore, the synthesis of superparamagnetic nanoparticles with an expected size distribution and stability of suspension is no

longer the biggest challenge for researchers. The key issue for *in vivo* or *in vitro* applications of superparamagnetic nanoparticles is becoming how to achieve the aim of stealth of these particles in the blood circulation and to attach them on desired sites.

2.5 Surface Modification

All magnetic nanoparticles are metal-based core material, and the particle surface would be exposed to a biological environment and oxidised during application if the bare particles were used directly. This could damage structures of the particles and destroy the magnetic property of the nanoparticles as well (Harris et al., 2003). On the other hand, nanoparticles in solid-phase cannot be injected into human bodies. Before injection, nanoparticles have to be dispersed to hydrophilic solvent via specific interaction between the nanoparticle surface and surfactants (Harris et al., 2003). Therefore, to implant nanoparticles into the human body, the method of treatment of the particle surface must be addressed. Coating the nanoparticles with biocompatible and hydrophilic surfactants is an effective way to achieve this.

There is another important role of surfactants on superparamagnetic nanoparticles. As mentioned in the previous section, when the ferrofluid is injected into human body as a MRI contrast agent, these nanoparticles must locate the targeting area accurately and rapidly. Appropriate surfactant or functional attachment of surfactant could achieve such objective. Some experiments *in vitro* already proved folate-mediated nanoparticles composed of PEG / poly ε-caprolactone (PCL) have potential of tumor cell-selective targeting, but there is a lack of *in vivo* experiments (Gee et al., 2003).

Hartley et al. (2001) reported a study on understanding the characteristics of the dextran coating. The research group has successfully immobilized the carboxymethylated dextran on the flat silica wafer via a polyethylenimine (PEI) interlayer. Their study shows that dextran could have strong covalent bonding on amine-rich surface. In addition, the same group of people have examined capability of protein adsorption of carboxymethylated dextran coating on the previous flat model at later time (Griesser et al., 2002). In the recent study, they have also tried two dextrans with different ratios of carboxyl to anhydroglucopyranoside ring, 1:2 and 1:30, and demonstrated that dextran with less carboxyl groups has better capability of resistance to protein adsorption.

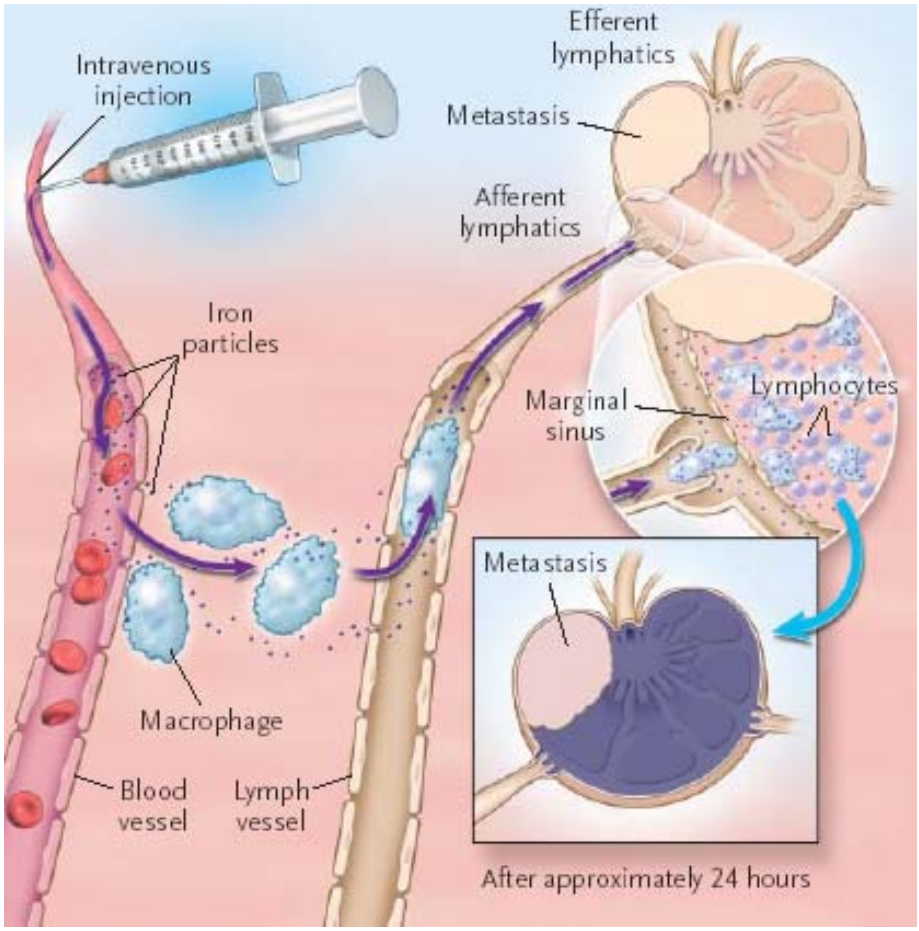

Figure 2-2: Sketch of in vivo application of lymphotropic superparamagnetic nanoparticles (Harisinghani et al., 2003)

Harisinghani et al. (2003) presented lymphotropic superparamagnetic nanoparticles, which they found can slowly extravasate from the blood vessels because the particle core, iron oxide, is coated with a dense packing of dextrans. These nanoparticles encapsulated by macrophages will finally reach the lymph nodes. A clinical experiment was successfully conducted on 80 cancer patients and clearly shows the potential of superparamagnetic nanoparticles for detecting tumors smaller than 1 cm. Harisinghani's study provides a useful experimental ground that the dextran coating could efficiently avoid phagocytosis of RES and prolong the blood circulation time of nanoparticles.

PEG and PEG-containing copolymers have been widely investigated for bio-applications. Kim et al. (2002) immobilized MPEG directly onto an iron oxide particle surface, and obtained PEG coated particles with a size distribution of approximately 200 nm but with many clusters of several single particles. The particles were prepared by co-precipitation technique. The same research group improved procedure of the MPEG coated particles down to around 8 nm

observed by TEM in their subsequent work (2004).

Moreover, Zhang and Zhang (2005) have used a conjugation of PEG and Folic acid (FA) to modify the magnetite nanoparticle surface through a (3-aminopropyl)-trimethoxylsilane (SAM) interlayer, which provides active amine groups to react with carboxyl groups on PEG molecules. In this study, they also found the high quantity of intracellular uptake of these particles by the *in vitro* culture of human breast cells (BT-20).

As the researchers were already capable to synthesize superparamagnetic nanoparticles as small as only a few nm, surface modification becomes more important for using these particles for bio-applications. Except for dextran and PEG, there is a list of other substances, such as erythrocytes, liposomes, phospholipids, albumin and starch, could be utilized for bio-applications. However, dextran and PEG are more attractive to researchers, because of the approved resistance capability to protein adsorption and their functional derivatization (Mclean et al., 2000; Hartley et al., 2001; Griesser et al., 2002; Kingshott et al., 2002; Pasche et al., 2005[1,2]). These are the reasons for the popularity of dextran or PEG coated magnetic nanoparticles which could be applied for various *in vivo* and *in vitro* applications.

2.6 Summary

Many researchers are continuing to develop novel superparamagnetic nanoparticles, which can be used as magnetic agents in MRI. Superparamagnetic nanoparticles, which were coated by biocompatible hydrophilic surfactant, have been the focus of these studies. Various studies using different methods have already gained good results (Burke et al., 2001; Puntes et al., 2001; Gee et al., 2003; Harisinghani et al., 2003; Harris et al., 2003; Liz-Marzan, 2004; Abu Mukh-Qasem et al., 2005; Gupta et al., 2004). Aqueous co-precipitation technique, thermal decomposition, microemulsions technique and sonochemical method are all possible methods for nanoparticle preparation that have been developed and optimized in the last few decades. The smallest particles were 1-2 nm (Santra et al., 2001). Currently, many of the studies focused on surface modification, and used particles prepared by co-precipitation technique, which is the most commonly used method for magnetic nanoparticle synthesis. The applications of the particles using other methods, such as the non-aqueous route, have been limited by poorly engineered surfaces, even with excellent particle size distribution, shape, dispersion status and simpler synthesis procedure. However, stabilization and functionalization of the particles are the real challenge, for *in vivo* or *in vitro* applications, to avoid rapid elimination by RES. Furthermore, controllable surface of the mono-dispersed superparamagnetic nanoparticles were not developed by any of the previous studies, although many of them were found suitable surfactant for stabilization and stealth of the particles. This study is presenting the procedure of the high quality suspension of superparamagnetic nanoparticles with well engineered surface by controllable functional groups, which either resist non-specific protein adsorption or allow specific protein attachment. Although the study has already had success in modification of the particles, the product is still need to be further tested both *in vitro* with cells and *in vivo* with animals or even patients, which are beyond the scope of the present study.

3 PROJECT OBJECTIVE

3.1 Significance and Innovation

One of the main strategies for treating cancer is based on the early diagnosis of tumors. When detected at an early stage, cancer can be treated with a higher success rate. MRI provides images with excellent anatomical detail and soft tissue contrast but the technique is relatively insensitive for the detection of mm-sized tumors and metastases. However, the sensitivity of MRI can be improved by using MRI contrast agents and improved acquisition techniques. In particular, the use of superparamagnetic nanoparticles holds considerable promise (Alexiou et al., 2000; Harisinghani et al., 2003). These nanoparticles contain a crystalline superparamagnetic metal or metal oxide core and are coated with a dense packing of biocompatible polymers to prolong their circulation time in the blood. They are usually taken up by lymph nodes in animals and humans. Because of the larger size of nanoparticles (approximately 10 nm diameter) of metals, such as iron and cobalt, and those of iron oxide, they potentially provide a much stronger magnetic force than conventional contrast agents based on the gadolinium ion (0.1 nm) containing colloids. In addition, although the particles consist of ferro magnetic materials, they are ferro magnetic only in an applied external field, such as in MRI. They are paramagnetic if a field is not applied, a phenomenon called “superparamagnetism”. The increased magnetic force of the particles provides an enhanced contrast and resolution of the magnetic resonance image, allowing metastases as small as 1mm to become visible. Although, this project was mainly focused on the study of the magnetic nanoparticles for MRI diagnosis, the other bio-applications with similar applied environment to these applications could also benefit from the development of such particles.

A significant aspect of the project was that it was performed in collaboration with the Ian Wark Research Institute (Prof. Peter Majewski) and the Royal Adelaide Hospital (Dr. Michael Brown), combining expertise in chemical engineering,

materials- and nano-science and clinical research. This interdisciplinary approach was a major strength.

This project produced the following outcomes:

- Identification of the optimum parameters to surface engineer monocrystalline superparamagnetic nanoparticles with biocompatible macromolecules such as dextran and PEG.

- Exhaustive characterization of the bio-interfacial properties of Dextran- and PEG-coated nanoparticles.

- Proof-of-principle of their conjugation with biomacromolecules such as monoclonal antibodies.

This research extended previous studies undertaken at the Nano- and Bio-Materials Centre at the Ian Wark Research Institute in collaboration with the Royal Adelaide Hospital, Adelaide University and the Sydney Cancer Council. The outcomes of this work are a further step in the development of optimal superparamagnetic nanostructures to help early detection of cancer.

3.2 Objectives

The scope of current project was to optimize the surface-engineering procedures of superparamagnetic nanoparticles. Monocrystalline iron oxide nanoparticles were coated with macromolecules such as dextran or PEG, in order to increase the colloidal stability, improve bio-interfacial properties and as a result increase the blood circulation time. To achieve this aim, the project was performed in six stages below:

i. Optimization of a dextran-coating procedures of iron oxide nanoparticles

ii. Optimization of a novel PEGylation procedure of iron oxide nanoparticles developed at the IWRI;

iii. Characterization of dextran-coated and PEGylated nanoparticles by transmission electron microscopy (TEM), X-Ray Photoelectron Spectroscopy (XPS) , Fourier Transform Infrared (FTIR) and Dynamic Light Scattering (DLS);

iv. Characterization of the bio-interfacial properties of dextran-coated and PEGylated nanoparticles in an *in vitro* protein adsorption model;

v. Investigation of the conjugation with bio-active macromolecules such as monoclonal antibody.

4 METHODOLOGY

4.1 Introduction

Researchers have used via various strategies to study superparamagnetic nanoparticles for biomedical applications. However, all studies in this area could fall into two main stages: particle synthesis procedure and surface modification. The present project aimed to go through these two main stages based on experience from previous studies.

As mentioned in the previous section, monocrystalline suspension of superparamagnetic nanoparticles was chosen in the present study. For this reason, synthesis procedures of both iron and iron oxide particles were studied to identify the most optimal route of synthesis of mono-dispersed nanoparticles. Three methods of nanoparticle synthesis were examined in the laboratory for this project. Iron is highly magnetic and would be expected to be superparamagnetic at nano-scale, but metal iron is not suitable for biomedical application because it oxidises quickly in aqueous solution, which has been demonstrated by preliminary experiment in the laboratory. Fe_3O_4 and γ-Fe_2O_3 are two typical iron oxide materials suitable for superparamagnetic nanoparticles. On the other hand, γ-Fe_2O_3 is the most stable compound because it only contains ferric cations and will not oxidise, but the synthesis procedures of γ-Fe_2O_3 are much more complicated.

A co-precipitation technique was investigated to further understand and optimize it for the present study. Following the experiments carried out by Gupta et al. (2004), the conditions of synthesis procedure were slightly adjusted. However, the overall reaction is described by the following equation (4-1):

$$Fe^{2+} + 2Fe^{3+} + 8OH^- \rightarrow Fe_3O_4 + 4H_2O\,. \qquad \textbf{(4-1)}$$

$$Fe_3O_4 + 0.25O_2 + 4.5H_2O \rightarrow 3Fe(OH)_3\,. \qquad \textbf{(4-2)}$$

Fe_3O_4 still contains ferrous cations, which have a high possibility of oxidation in an oxygen rich environment. This reaction is shown as equation (4-2). In order to confirm precipitation of the complete Fe_3O_4 nanoparticles, reaction conditions have to be well controlled while the reaction proceeds. Moreover, a quick surface modification with appropriate surfactants, such as poly(ethylenimine) (PEI), is the best way to avoid oxidation of Fe^{2+}. Preliminary experiments in the laboratory successfully generated magnetite nanoparticles with PEI coating, which efficiently prevent particles from oxidation, and precipitation caused by interaction between particles. However, aggregation takes place more rapidly as the particle suspension ages.

In order to overcome the drawbacks of the aqueous precipitation reactions, researchers have investigated non-aqueous routes. One of the non-aqueous routes reported by Pinna et al. (2005) overcomes the limitations of other non-aqueous routes and aqueous routes, and this was employed in the present study. Magnetite nanoparticles produced by reported route have a size distribution ranging from 12 nm to 25 nm with only environmentally friendly benzyl alcohol (BA) as a solvent as well as a ligand, making these particles more susceptible for biomedical application. A single surfactant, BA, was used in the reaction. BA is extensively used in the food industry because it is regarded as an environmentally friendly solvent, and is appropriate for synthesis procedures of many other metal oxide nanoparticles.

Dopamine

However, these nanoparticles need to be transferred to an aqueous solvent for bio-applications. Xu et al. (2004) found that 2-(3,4-dihydroxyphenyl)ethylamine (dopamine) could provide an excellent and robust anchor for iron oxide particles. As our preliminary experiment showed, dopamine produced stronger covalent bonding than oleic acid as an anchor on the surface of particles via a ligand exchange test. While hydroxyl (-OH) bonds on the surface, the amine groups ($-NH_2$) on the other end of dopamine formed a positively charged shell over the nanoparticles, which effectively prevents aggregation between these magnetic particles. The magnetite nanoparticles were stabilized in MilliQ water with dissolved dopamine as the solvent.

Suspension of magnetite nanoparticles with a dopamine coating provides an excellent stage for further surface modification with the aim of attaching functional groups for continuing derivatization and protecting the particles from rapid capture by the reticuloendothelial system (RES). In this study, two carboxylmethyl dextran and di-carboxyl-tailed PEG have been investigated as further immobilization molecules. $–NH_2$ groups provided by the dopamine coating easily reacted with –COOH groups on either dextran or PEG. This introduces another undesired problem, crosslinking, leading to massive aggregation of the particles and destruction of the stable suspension. Both dextran and PEG possess at least two or more –COOH groups on each of their long chain molecules, so that one of these molecules may bind to two or more particles if many particles surrounded it. Obviously, a possible solution is to increase the separation between the mono-dispersed particles. This is achieved by the use of a high concentration surfactant solution during the coating procedure to reduce the chance that one surfactant molecule meets two or more particles before the $–NH_2$ groups were reacted with –COOH groups on other molecules.

As it has been reported in many other studies, the dextran coating and the PEG coating produced efficient resistance to non-specific protein adsorption, especially given the slightly negatively charged surface induced by un-reacted $–COO^-$ groups in aqueous solution. Also, these $–COO^-$ groups offer an opportunity for further attachment of specific functional groups, such as monoclonal antibodies. In the present study, efficient non-specific protein adsorption resistance has been confirmed by demonstrating the resistance to two opposite surface charged proteins, albumin (from human) and lysozyme (from hen egg white).

Based on the ideas discussed above, a series of experiments has been completed in the IWRI laboratory. The following sections describe the details of these experiments and discuss the results of the experiments.

4.2 Synthesis Procedures of Nanoparticles

4.2.1 Electrolysis Method for Iron Nanoparticles

A commercially available generator, SilverGen (normally used to generate silver nanoparticles), was used to generate Fe nanoparticles. SilverGen can generate a stable aqueous dispersion of silver nanoparticles with a size distribution of 1 nm to 5 nm by using a constant current. Based on the principle of electrolysis, Fe nanoparticles were synthesised by replacing the silver electrodes with Fe electrodes (Figure 4-1). By contrast, a hydrophilic surfactant, PEI, solution in MilliQ water was used as solvent instead of MilliQ water during processing. The aim is to coat the particles with the surfactant to prevent particle oxidation in aqueous solution. The procedure required 24 hours with vigorously magnetic stirring.

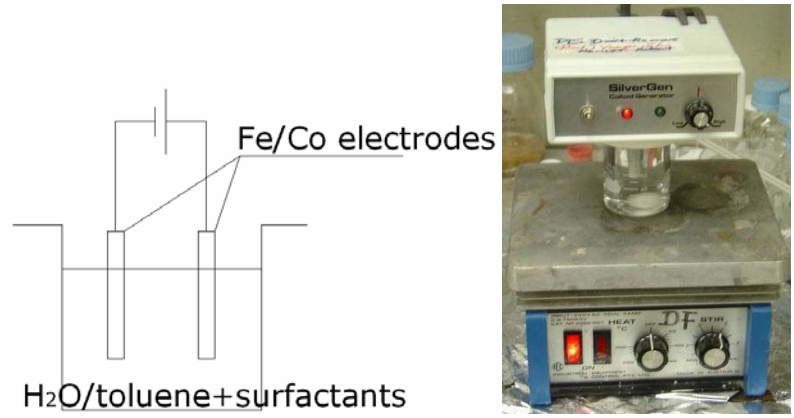

Figure 4-1: Sketch of the Generator (left) and the picture of the SilverGen (right)

4.2.2 Co-precipitation Technique for Magnetite Nanoparticles

2M Fe^{2+} and 1M Fe^{3+} chloride solutions were prepared by dissolving $FeCl_2.4H_2O$ and $FeCl_3.6H_2O$ in 0.5M HCl solution, respectively. These were mixed at molar ratio of 1:2. 0.5M NaOH and then preheated to 80ºC for 10 minutes as a base. The mixture solution was slowly added dropwise to the base of NaOH solution with bubbling N_2 gas and vigorous magnetic stirring. A black precipitate was produced immediately. Particles were washed with ethanol and MilliQ water, and

finally re-dispersed in MilliQ water. During washing, a permanent magnet was used to assist collection of the magnetic black precipitate.

In comparison, in order to stabilize the particles with PEI coating, the black precipitate was washed with ethanol instead of MilliQ water and treated with 5 mg/mL PEI with vigorous magnetic stirring overnight. These particles were then redispersed in MilliQ water.

4.2.3 Non-aqueous Method for Magnetite Nanoparticles

For reducing O_2 and H_2O, in a glove-box under nitrogen atmosphere, 500 mg of iron (III) acetylacetonate ($Fe(acac)_3$) powder was mixed with 10 mL of benzyl alcohol. The reaction mixture was sealed in a Teflon cup which was then carefully placed and tightly sealed into a steel autoclave. The steel autoclave was transferred from the glove-box to a furnace, preheated to 175ºC and kept at 175ºC for 48 hours. Then, the sample cooled to room temperature in air. The resultant dark brown suspension was kept for further study and analysis purposes.

4.3 Surface Modification

This section describes the continuing study on the Fe_3O_4 nanoparticles produced by the non-aqueous method. After synthesis, the particles were dispersed in BA. As the final product was designed for biomedical application, the sample must be transformed into an aqueous ferrofluid. Subsequent experiments attempted to immobilize the particle surface with dopamine, carboxymethylated dextran and PEG as functional molecules. As well, non-specific protein adsorption prevention and specific antibody attachment tests were performed on the modified surface to reveal the chemical characteristics of the dextran and PEG coatings.

4.3.1 Ligand Exchange Procedure

As the initial step of the further surface modification procedure, dopamine was chosen as the ligand to exchange the nanoparticles from organic solvent, BA, to an aqueous solvent.

A ligand exchange procedure was used to capture the nanoparticles with the enediol ligand, dopamine. The black particle suspension in benzyl alcohol was mixed with 10 mg/mL dopamine solution in MilliQ water at the same volume mixing ratio. A 10-minute sonication, which was followed by half-day settling, was given to the mixture. The nanoparticles transferred from the organic layer, BA layer, to the aqueous layer, dopamine solution layer. The aqueous phase was collected and washed with ethanol three times using centrifugation at 14,000 rpm to remove un-reacted excess dopamine. The particles were finally redispersed in MilliQ water with assistance of sonication.

4.3.2 Grafting of Carboxymethyl Dextran

4.3.2.1 Preparation of Carboxymethyl-dextran

Carboxymethyl dextran has been synthesized based on the procedure

previously reported (Griesser et al., 2002). Typically, 10 g of dextran was dissolved in 2M NaOH solution containing bromoacetic acid. The extent of derivatization was controlled by the amount of bromoacetic acid. Two carboxymethyl-dextrans were prepared and used in this study: carboxyl to anhydroglucopyranoside ring ratios of 1:2 and 1:10. The products were purified by extensive dialysis and recovered using freeze-drying.

4.3.2.2 Grafting Procedure

The dopamine modified particles were redispersed in MilliQ water. Carboxymethyl dextran solutions were prepared by dissolving the polymers (10 mg/mL) in MilliQ water and adjusting the pH to 8.5 and agitated for 1 hour. The suspension of particles fractionated by size using centrifugation was added dropwise to 10 mg/mL dextran solutions under vigorous agitation. The volume of the dextran solutions was twice to the volume of particle suspension. The reaction mixture was agitated for 1 hour after which N-(3-Dimethylaminopropyl)-N'-ethylcarbodiimide hydrochloride (EDC) and *N*-Hydroxysuccinimide (NHS) solution in MilliQ water were added dropwise to reaction mixture while agitating to activate carboxyl groups for the reaction. The grafting reaction was allowed to proceed for 2 hours. The particles were then washed with MilliQ water three times using a 14,000 rpm centrifuge. This procedure was utilized for both carboxymethyl-dextrans.

4.3.3 Grafting of Carboxyl PEG

4.3.3.1 Direct Grafting PEG on Dopamine Coating at Room Temperature

10 mg freeze-dried PEG powder was dissolved in 1 mL dimethyl sulfoxide (DMSO), and carboxylate (-COOH) groups were activated by NHS and *N,N'*-dicyclohexylcarbodiimide (DCC) only 5 minutes in advance. PEG solution was added dropwise to the particle suspension in DMSO with vigorous agitation. Reaction lasted for overnight with agitation. After reaction, the particles were washed with ethanol three times using centrifugation.

4.3.3.2 Epichlorohydrin Pre-treatment

The suspension of dopamine coated particles, which was used for carboxyl PEG coating were washed only with absolute ethanol three times and redispersed in absolute ethanol after ligand exchange procedure to reduce the O_2 and H_2O during the following experiments.

Experiment was performed in a glove-box under nitrogen atmosphere. Dopamine coated particles were washed with epichlorohydrin once to remove most of the ethanol solution and then redispersed in epichlorohydrin by quick sonication. Derivatization of dopamine with epichlorohydrin was allowed for 2 hours, and the particles were washed with and redispersed in absolute ethanol for grafting procedure of carboxyl PEG.

4.3.3.3 Melting Procedure for Grafting PEG

100 mg of Carboxyl PEG was melted at 95ºC and dissolved in 2 mL of absolute ethanol per mL of suspension of dopamine coated particles in a glass tube. The particle suspension was added quickly but dropwise to the PEG solution with sonication for a further minute. The reaction mixture was kept at 95ºC for 12 hours. The resultant sample was washed with ethanol three times using centrifugation.

Carboxyl PEG (MW=3,400, g/mol), carboxyl PEG (MW=600, g/mol) and mPEG-NH_2 were the three PEG investigated by the same procedure in this stage. The latter two PEG were studied in comparisons to the first one.

4.3.4 Protein Adsorption

Experiments at this stage were carried out with both dextran coated particles and PEG coated particles. All the samples were washed three times with and redispersed in Phosphate Buffered Saline (PBS), and processed through the same procedure of protein adsorption.

4.3.4.1 Non-specific Protein Adsorption Resistance

A protein solution of albumin and lysozyme in PBS (0.5 mg of albumin and 0.5 mg of lysozyme per 1 mL of PBS) was prepared and mixed gently with the same volume of PBS suspension of nanoparticles at room temperature (RT). The nanoparticles were exposed to the protein solution for 60 minutes and washed with PBS twice, MilliQ water twice and ethanol twice, and removed free and weakly adsorbed proteins by centrifugation. Alternatively, the remaining carboxyl groups on the dextran backbone or the other end of PEG were activated by EDC and NHS solution and the particles were exposed to the same protein solution after quick removal of excess of the EDC and NHS in the solution by centrifugation. The nanoparticles were then dried and mixed with dry KBr powder and analyzed using DRIFT-IR spectroscopy.

4.3.4.2 Antibody Attachment

Compared to our estimate of the mass of polymer coated particles, a 5 times excess amount of the antibodies was dissolved in the physiological buffer of pH 8.5, and well mixed with the particle suspension in the same buffer, which was followed by activation of carboxyl groups by EDC and NHS solution. The reaction time was 2 hours. The particles were washed three times with the buffer assisted by the magnetic field from a permanent magnet.

4.4 Characteristic Measurement

Particle structure was investigated by Transmission Electron Microscopy (TEM) and Dynamic Light Scattering (DLS). X-ray Photoelectron Spectroscopy (XPS) and Fourier Transfer Infrared (FTIR) were employed to analyze components on the particle surface. Standard curve of absorbance of Prussian blue of particle suspension by UV-Visible Spectroscopy (UV-Vis) was used to estimate the concentration of magnetite nanoparticles.

4.4.1 Transmission Electron Microscopy (TEM)

A Philips CM100 Transmission Electron Microscope in Microscopy of Adelaide University was utilized for analysing the structure of the nanoparticles. The images were made with appropriately diluted particle dispersion in MilliQ water. The samples were dropped on carbon-coated copper grids and dried in air at RT.

4.4.2 X-ray Photoelectron Spectroscopy (XPS)

A Kratos Axis Ultra X-ray Photoelectron Spectroscope in the IWRI laboratory was used to analyse the chemical characteristics on the particle surface. The survey spectra were collected between 1100 and 0 eV. The C 1s high resolution analyses were also made for further understanding of the samples. The samples were prepared on gold-coated silicon wafers, ethanol dispersion of particles was dropped and dried onto 2 mm x 2 mm gold-coated silicon wafers at RT.

4.4.3 Fourier Transform Infrared (FTIR)

A Nicolet Magna-IR 750 spectrometer (Thermo Electron Corporation, Massachusetts, USA) was used to characterize surface chemical functionality. Spectra were collected between 4000 and 400 cm^{-1} at a resolution of 4 cm^{-1}. Background measurements were performed with ground KBr powder before the analysis of every batch of samples. The sample measurements were performed

with ground powder mixture of KBr powder and dried particles. H_2O in all samples and backgrounds were reduced by heating at 90~95ºC for 1 hour in advance.

4.4.4 Dynamic Light Scattering (DLS)

A Zetasizer Nano ZS Dynamic Light Scattering by Malvern Instrument Ltd. was used to measure dynamic size distribution as well as the zeta potential of the nanoparticles. The samples were appropriately diluted and filled into a specific unique Zeta potential cell for the Zetasizer Nano ZS (shown as left). Both size distribution and zeta potential were measured with the same cell at the same time.

4.4.5 Fe Determination by UV-Vis

The iron content of the nanoparticles was determined using Prussian blue titration and atomic absorption spectroscopy by a CARY 1E UV-Visible Spectrophotometer. Standard curve was prepared using $FeCl_3.6H_2O$. Absorbance was read at 690 nm. Nanoparticles suspensions were treated with hydrochloric acid. The mole concentration of iron oxide magnetic nanoparticles was estimated from the iron concentration of particle suspension and the size-distribution from TEM and DLS. The amounts of other chemicals participated in reactions of every stage were estimated based on this calculation.

4.4.5.1 Standard Curve of Fe^{3+} Concentration

Standard curve of iron concentration was portrayed with absorbance at 690 nm of mixture solution of Fe^{3+} standard solutions and potassium ferrocyanide ($K_4Fe(CN)_6$) solution. The procedure of preparation described as below.

Three solutions were prepared in advance:

- 0.5M HCl solution

- 1.5mM, 1mM, 0.75mM, 0.5mM, 0.25mM, 0mM Fe^{3+} standard solution in 0.5M HCl solution
- 5 wt.% aqueous (MilliQ water) solution of potassium ferrocyanide ($K_4Fe(CN)_6$)

The standard solution was settled for 1 hour, and then mixed with 5 wt% $K_4Fe(CN)_6$ solution at ratio of 1:1 in cells of UV spectrophotometer. After another 10 minute settling, the mixture was analysed and the absorbance was read at the wavelength of 690 nm. The data was processed and the standard curve for Fe determination was provided as shown in Figure 4-2.

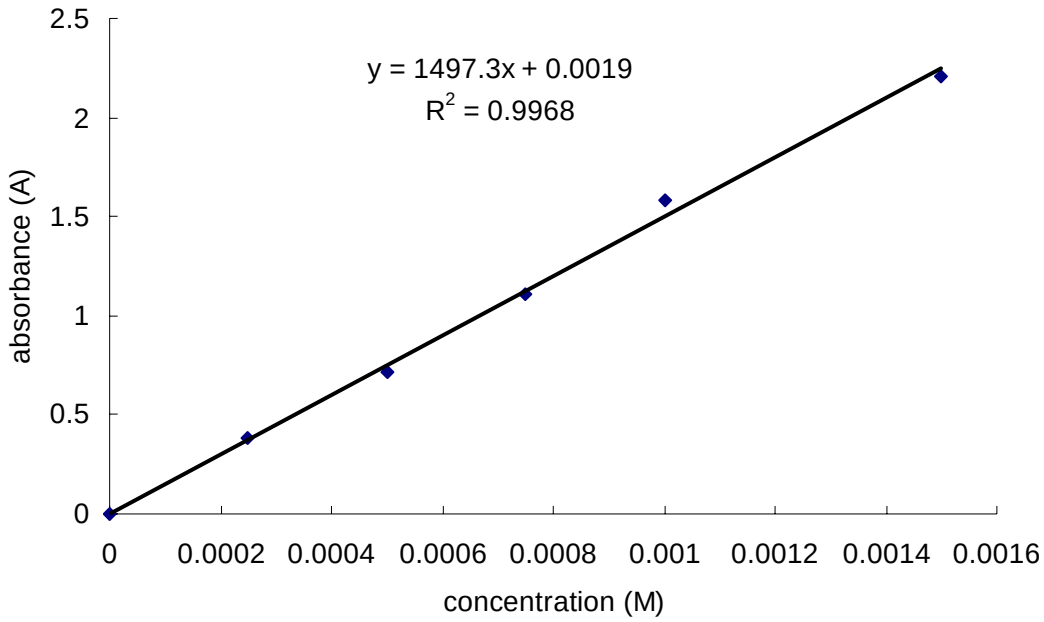

Figure 4-2: Standard Curve of Fe^{3+} Concentration

The expression:

$$y = 1497.3x + 0.0019 \quad \textbf{(4-3)}$$

Where *y* is absorbance of the samples at 690 nm,

x is the Fe^{3+} concentration reading value on standard curve.

5 RESULTS AND DISCUSSION

5.1 Introduction

The main objective of the present study was to produce superparamagnetic nanoparticles with a narrow size distribution and monocrystalline dispersion of the particles. Iron-based materials, as the magnetic materials, have been investigated by three different routes to determine the most suitable route for further study of surface modification for biomedical application purposes. The magnetite nanoparticles by non-aqueous route were compared with those by co-precipitation technique, and the former method was found to be a more appropriate procedure for the current study, although these methods have already been studied by various researchers as single cases. However, further surface modification is the new focus of this study. Two types of carboxymethyl dextran and carboxyl tailed PEG were considered as functional molecules to immobilize the particle surface in aqueous solvent. Non-specific/specific protein adsorption test were carried out on these coating to determine chemical characteristics of the coatings. FTIR, XPS, DLS and TEM were employed in an attempt to better understand several aspects of these coatings such as size distribution, surface charge, particle structure, chemical characteristics and suspension performance.

5.2 Synthesis Procedures

5.2.1 Electrolysis Method

Because Fe is a very strong magnetic material, its stability in aqueous solvent is very poor when there is no protection of appropriate surfactants on its outer layer. As mentioned previously, the electrolysis method was undertaken here as the preliminary study. The particle suspension generated by the SilverGen was analysed by TEM. Results from TEM shows that these particles would aggregate immediately in solvent after synthesis where MilliQ water with no surfactant was present. Iron is not stable in an oxygen-rich environment as a simplex element. In pure aqueous solvent, the surface of Fe particles is rapidly oxidized to form iron-based compounds, such as goethite (FeO(OH)) which exhibit non-magnetic properties (Figure 5-1). On the other hand, when PEI was mixed with MilliQ water as a solvent for electrolysis, particle formation was not observed by either TEM or naked eye after 24 hours electrolysis at room temperature. This could be due to the surfactant coating the iron electrodes and preventing the separation of iron particles from one of the electrodes.

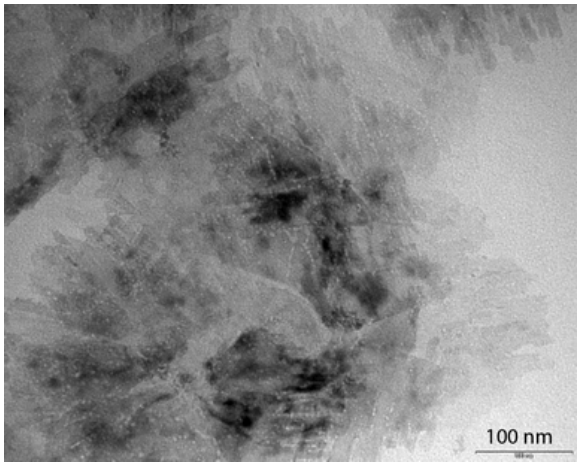

Figure 5-1: TEM image of nanocrystals by electrolysis method

However, iron oxide appears to be much more stable than metal iron in an aqueous solution, which provides the chance to further coat the particles with surfactant to modify the surface properties. In addition, using iron oxide as particle core proved to be a simple and effective method for preparation of the nanoparticles for bio-applications.

5.2.2 Co-precipitation Technique versus Non-aqueous Method

Black precipitate formed immediately as ferric and ferrous chloride salt solution was added to NaOH at 80ºC. This method is known as co-precipitation technique. Figure 5-2 shows the TEM images of these particles where a size distribution was observed to be between 15 nm to 50 nm. This result is in agreement with previous studies (Gupta et al., 2004). These particles were easily harvested using a strong magnet. Upon washing with PEI, the particles were stable in a suspension of MilliQ water for approximately 2 hours. However, most of the PEI coated particles precipitated after 12 hours, although a small amount of these particles was still well dispersed in solvent. TEM images (Figure 5-2) affirmed this observation where only a small amount of particles was remained mono-dispersed in solvent. The surrounding gray fog-like area as shown in Figure 5-2b on the bottom left image of Figure 5-2 could be attributed to the excess surfactant in the solution, which prevented particles from agglomerating caused by the interaction between particles.

Figure 5-3 shows the nanoparticles produced by the non-aqueous route. Particles dispersed similarly to those in figure 5-3 and were produced at a high yield. These particles were almost perfect spheres with a size distribution ranging from 15 nm to 30 nm. Without further surfactant treatment, most of the individual particles tended to form small agglomerates (Figure 5-3a), which were suitable for further surface modification. These agglomerates could be broken easily by sonication during ligand exchange with hydrophilic dopamine solution. The dopamine coated particles as shown in Figure 5-3b were mono-dispersed. The particles repelled each other, thus indicating the presence of the $-NH_2$ of the dopamine coating positively charged the surface of these nanoparticles.

Compared to co-precipitation technique, the non-aqueous route is much simpler. More importantly, this route provides particles that are of extremely high quality with narrow size distribution, spherical shape and monocrystalline habitat in BA. This method also offers a possibility of higher density and better quality of attachment of other functional molecules.

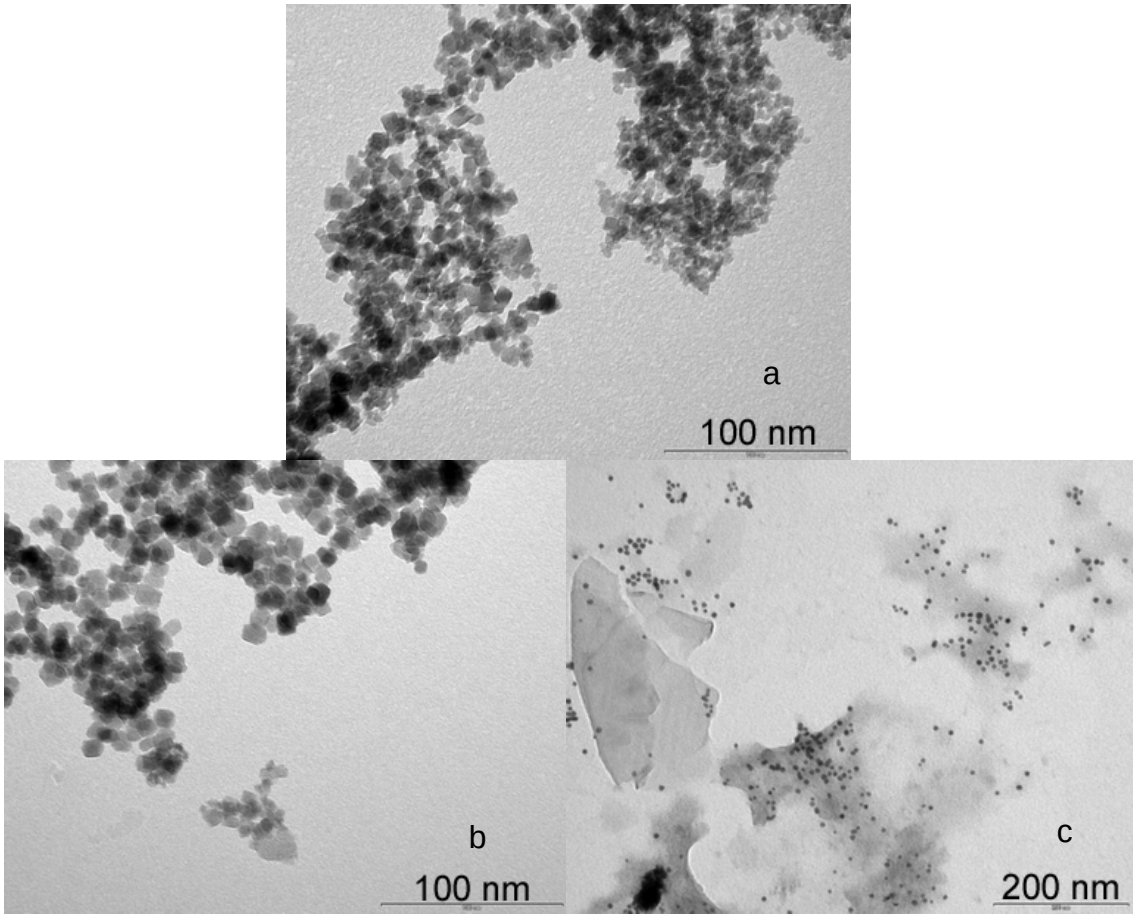

Figure 5-2: TEM images of particles by co-precipitation technique without PEI washing (a), particles with 20-hour PEI treatment in most area on grid (b) and particles with 20-hour PEI treatment in some area on grid (c)

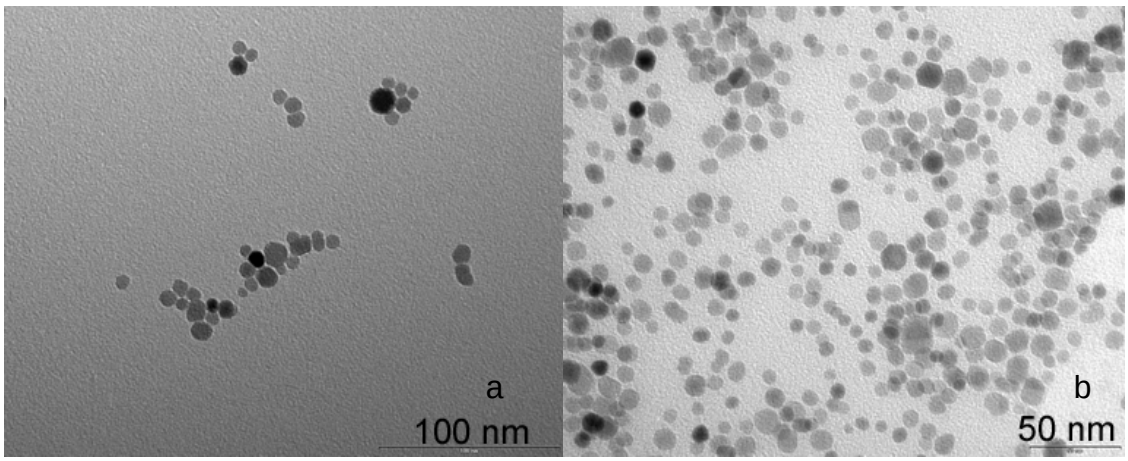

Figure 5-3: TEM images of bare particles by non-aqueous route without any coating (a) and the particles by non-aqueous route with dopamine coating (b)

5.3 Dopamine Coating

A large yield of monocrystalline magnetite nanoparticles with a size distribution between 15 nm and 30 nm as shown by TEM were obtained (Figure 5-3). The ligand exchange procedure with dopamine proceeded easily and subsequent aggregation of the nanocrystals was not observed in MilliQ water. Bidentate enediol ligands, such as dopamine, have been shown to be excellent capping agents for iron oxide nanostructures.

Furthermore, a ligand exchange procedure was used to demonstrate that dopamine provides a better ligand than carboxylic acid. This was carried out as follow: nanoparticles protected with oleic acid in hexane were mixed with an aqueous dopamine solution. After a few minutes of strong agitation, the dopamine ligand displaced the oleic acid molecules as shown by transferring the nanoparticles to the aqueous phase (Figure 5-4).

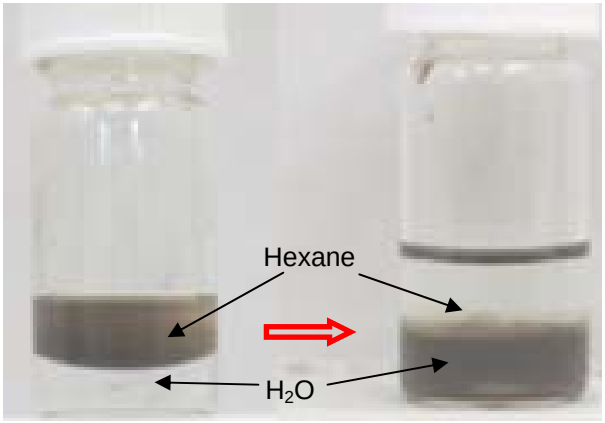

Figure 5-4: Ligand exchange between oleic acid and dopamine

Moreover, dynamic light scattering (Figure 5-11) indicated a mean volume distribution of about 27 nm in agreement with size distribution observed in the TEM images (Figure 5-3). The dopamine coated nanoparticles were stable in water due to the electrostatic stabilization of the amino groups as confirmed by zeta potential measurements. A zeta potential of 60 mV in MilliQ water as shown in Figure 5-9, indicates the amine groups of dopamine positively charged the surface of the magnetite nanoparticles.

5.4 Dextran Coating

5.4.1 Carboxymethylated Dextran

By varying the amount of bromoacetic acid, dextran could be carboxymethylated with different ratios of carboxyl groups per anhydroglucopyranoside ring. In this study, two different ratios of carboxyl groups per anhydroglucopyranoside ring were produced and analysed by titration and FTIR (Figure 5-5). The significant increase of peaks at around 1750 cm^{-1} on both spectra of dextran(1:2) and of dextran(1:10) present the C-O bonding from –COOH groups, and the different ratios of –COOH groups to one dextran molecule were proved by varied signal rising multiples.

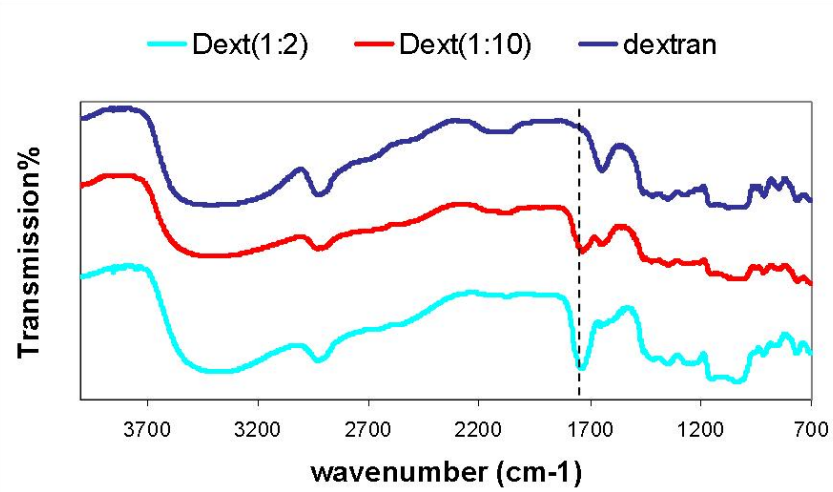

Figure 5-5: FTIR spectra of pure dextran; dextran(1:10) and dextran(1:2)

5.4.2 Grafting of Two Carboxymethyl Dextran

The next step was to covalently attach the carboxymethyl dextran to the amine of the dopamine ligand using carbodiimide chemistry. To minimize bridging between nanoparticles by the dextran macromolecules during the coating procedures, low molecular weight dextran were used (15,000 to 20,000). The nanoparticles suspension was slowly added under vigorous agitation to the dextran solutions and maintained agitating at the same speed for one hour. Previous works (Hartley et al., 2001; Harisinghani et al., 2003; Bautista et al.,

2005; Hong et al., 2005) have shown that meticulous choice of experimental conditions allows the aggregation-free coating of nanoparticles with polyelectrolytes. EDC and NHS were then added to the mixture to covalently immobilize the dextran onto the particles. After three washing using centrifugation, the nanoparticles could be resuspended in a physiological buffer. Chemical analyses were performed using XPS (Figure 5-7). Survey spectrum (see APPENDIX A) showed significant changes in the iron to carbon ratio confirming the grafting of the dextran macromolecules on the nanoparticles (0.17 for dextran(1:2) and 0.05 for dextran(1:10) in comparison to 0.66 for dopamine coated nanoparticles). Determining the thickness of the dextran layers using an XPS overlay model was not attempted as the roughness of the particles dried onto gold-coated silicon wafers was expected to induce too much error to provide accurate values. However, the decrease of the ratio of the iron to carbon between the dextran(1:2) coating and the dextran(1:10) coating, from 0.17 to 0.05, supports a possible deduction, that the dextran(1:10) coating could form a thicker shell structure than the dextran(1:2) coating due to the longer flexural molecule chain between two covalent bonding by carboxymethyl groups and amine groups on the particle surface. Figure 5-6 illustrates the possible structures of dextran(1:10) and dextran(1:2) on the dopamine coated nanoparticles.

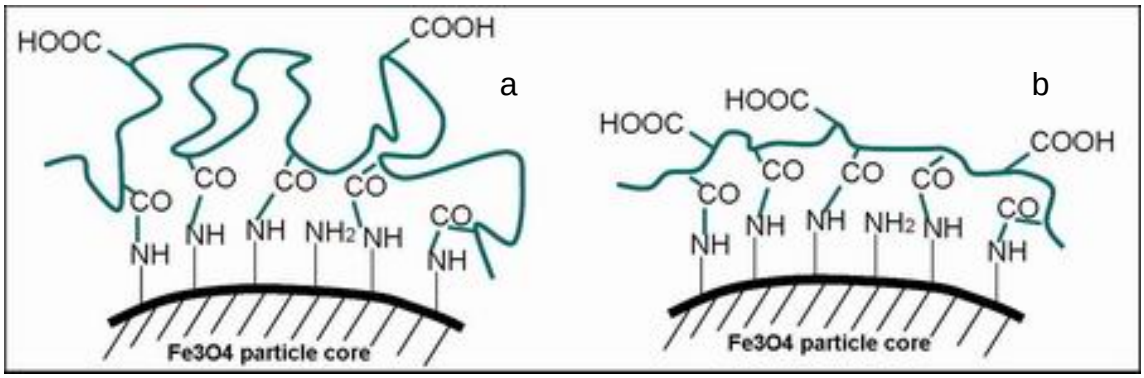

Figure 5-6: Sketch of possible deduction of structures of dextran(1:10) coating (a) and dextran(1:2) coating (b)

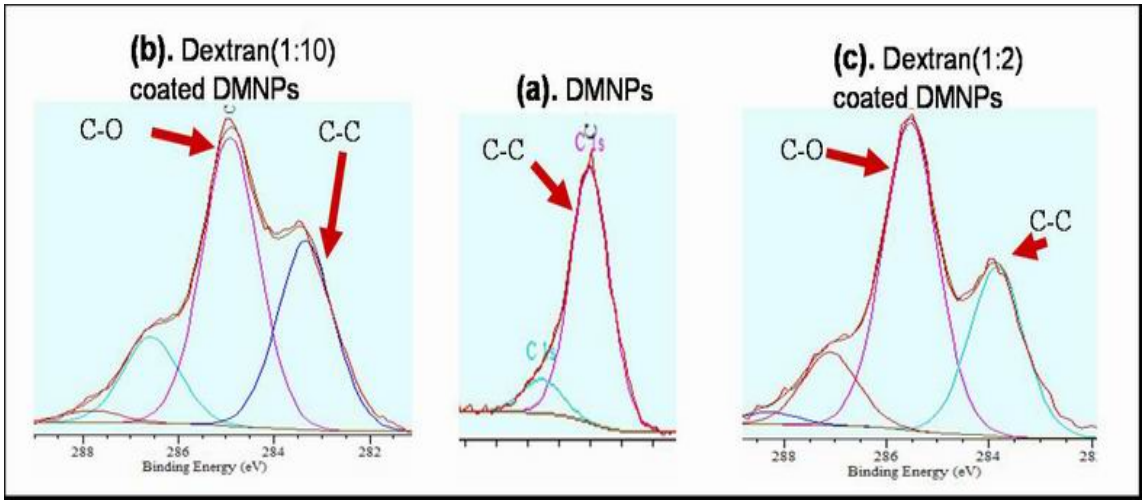

Figure 5-7: High-resolution XPS (a) C1s of dopamine coated nanoparticles, (b) C1s of dextran(1:10) coated nanoparticles and (c) C1s of dextran(1:2) coated nanoparticles.

The presence of dextran on the particles was also confirmed by C 1s high resolution analysis. Both dextran-coated nanoparticles displayed a significant increase in the component at 286 eV of the C 1s attributed to the C-O bonds from the anhydroglucopyranoside ring (Figure 5-7).

One of the major challenges in the surface modification of nanoparticles is to avoid aggregation during the coating procedure. It is even more challenging in the case of magnetic nanoparticles where dipole-dipole interaction between single nanoparticles must be considered in addition to van der Waals forces.

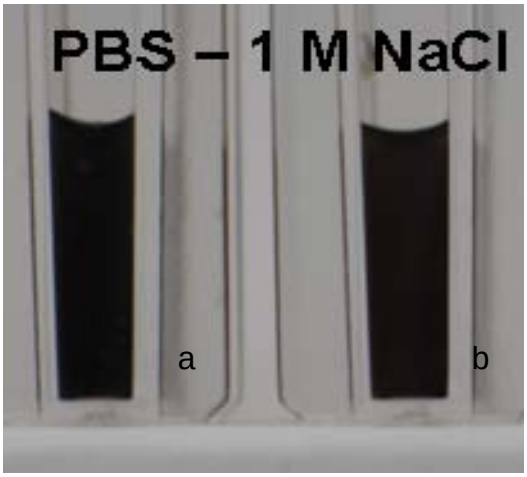

Figure 5-8: Stability of Dextran coated nanoparticles in PBS with high ionic strength (a: Dex(1:10); b: Dex(1:2)).

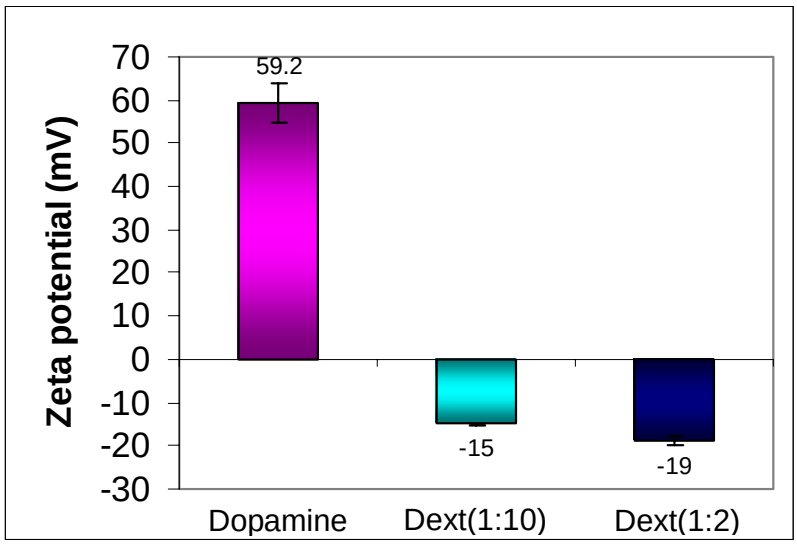

Figure 5-9: Zeta potential of dopamine coating in MilliQ water, dext(1:10) coating in PBS and dext(1:2) coating in PBS by DLS analysis

The coating procedure described here has been optimized to prevent such aggregation and subsequently, the dextran coated nanoparticles could be easily resuspended into PBS and remain stable even at high ionic strength (Figure 5-8). Zeta potential measurements indicated a slightly negative charge in agreement with excess carboxyl group present on the surface of the nanoparticles (-15 mV for dextran(1:10) and -19 mV for dextran(1:2)).

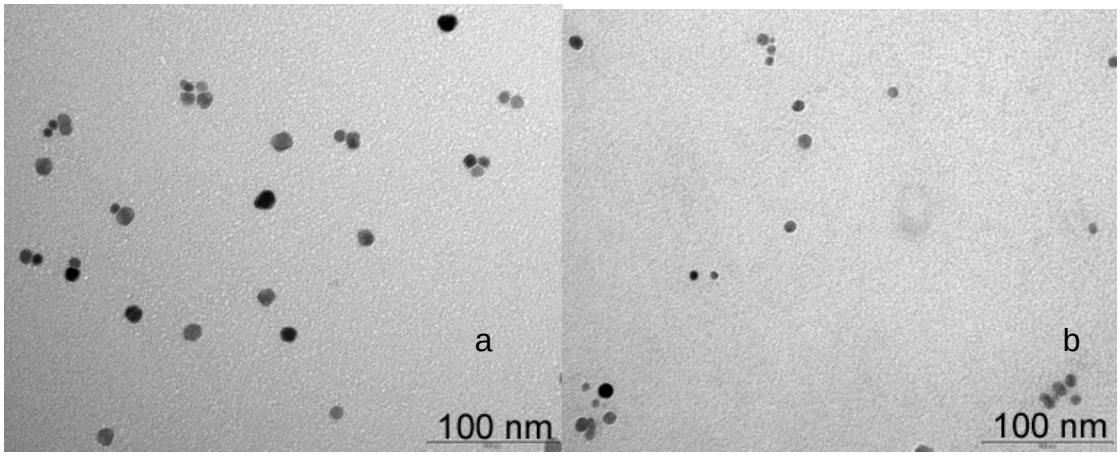

Figure 5-10: TEM images of dextran(1:10) coating nanoparticles (a) and dextran(1:2) coating nanoparticles (b)

The stability of the nanoparticles in high ionic strength solution could be attributed to the steric repulsion, thus preventing the iron oxide cores from aggregating. As shown in Figure 5-10, TEM measurements indicated zero or minimal aggregation of the nanoparticles. This was confirmed by the volume distribution determined by DLS that showed good mono-dispersity with only

minimal increase in the hydrodynamic diameter of the nanoparticles (Figure 5-11). However, a broadening of the distribution for the dextran(1:2) coated nanoparticles was observed. This could be due to the presence of some small aggregation of these nanoparticles, which also confirmed the supposition that the much thicker dextran(1:10) coating is better at preventing aggregation than the dextran(1:2) coating. Similar results were obtained for gold nanoparticles (data shown in APPENDIX B). More carboxyl groups on the dextran(1:2) available for electrostatic cross-linking of the dopamine coated nanoparticles during the coating procedures could explain the difference observed between the two carboxymethylated dextran.

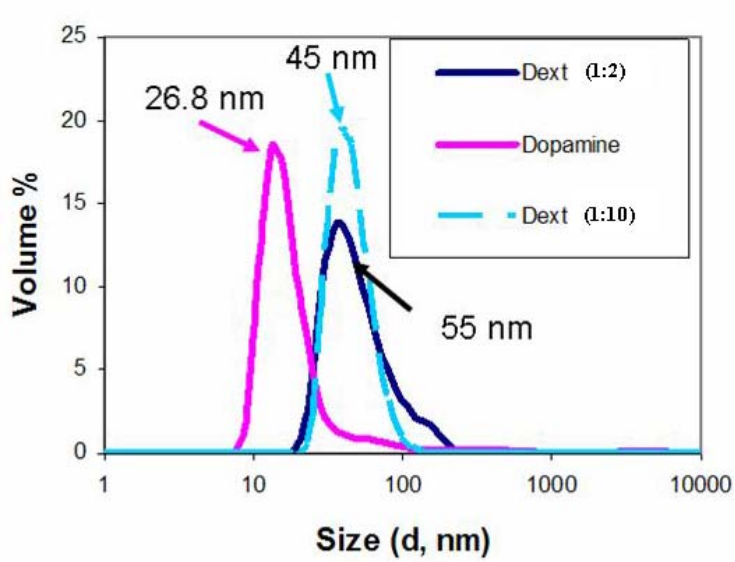

Figure 5-11: Volume size distribution of dopamine coating, dext(1:10) coating in PBS and dext(1:2) coating in PBS by DLS analysis

5.5 PEG Coating

5.5.1 Directly Grafting PEG on Dopamine Coating

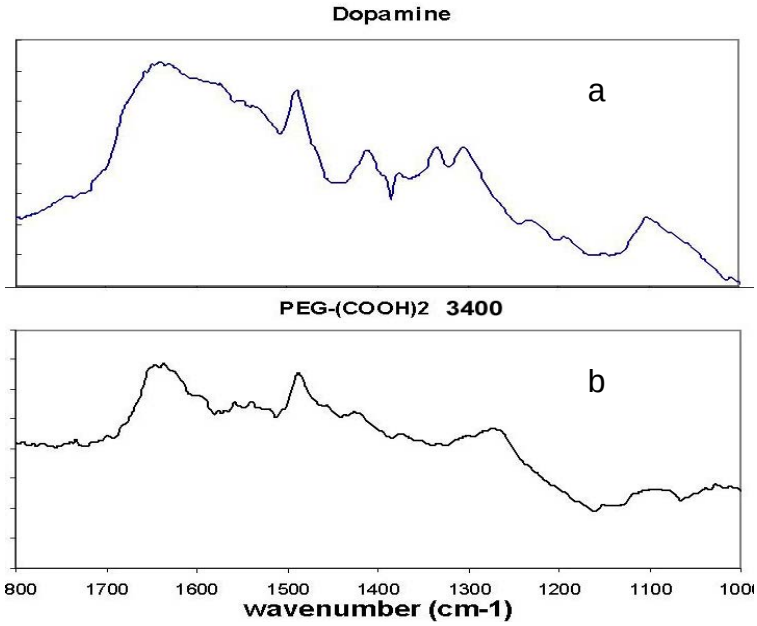

Figure 5-12: Comparison of FTIR spectrum of (a) dopamine coating with (b) PEG-$(COOH)_2$ 3400 coating without derivatization

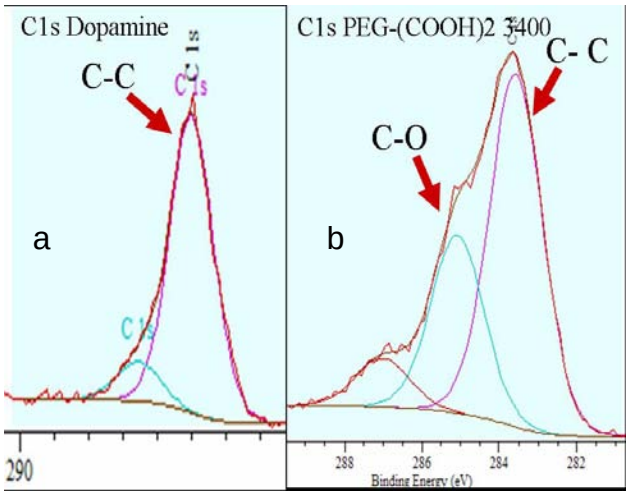

Figure 5-13: XPS C 1s high resolution analyses of (a) dopamine coating and (b) PEG-$(COOH)_2$ 3400 coating without derivatization

Similar procedure on dextran coating has been investigated on PEG-$(COOH)_2$ 3400 coating where carboxyl tailed PEG covalently bonded directly to amine groups in order to immobilize the PEG molecules on the surface of dopamine coated particles. As shown in Figure 5-12, no specific evidence from FTIR spectrum indicated the presence of PEG and –COOH groups. The XPS C 1s

high resolution spectra (Figure 5-13) revealed only a small increase in the component at 286 eV which attributed to the C-O bonds from PEG molecules. In addition, upon activating the –COOH groups on the surface of these particles, poor stability was observed in PBS and other high ionic strength. Hence, a PEG coating of such poor quality would not be suitable for *in vivo* application as a MRI contrast agent.

5.5.2 Grafting PEG by the Melting Procedure

Before immobilizing the PEG on the dopamine coating, epichlorohydrin, as the derivative of the dopamine, was allowed to react with dopamine coated particles to increase the reaction probability. Considering the steric feature of PEG-$(COOH)_2$ molecules, the steric hindrance could inhibit efficient reaction between –COOH groups and $–NH_2$ groups. Pulsed plasma is used to functionalize surfaces with reactive epoxy groups. In the present study, dopamine coated particles were in contact with epichlorohydrin with reduced O_2 and H_2O by the glovebox under nitrogen, such environment encourages the amine groups to react with chloromethyl groups so that the epoxy could be available for next step of grafting of carboxyl tailed PEG. After functionalization by epichlorohydrine, these particles were exposed to melted PEG. Figure 5-14 shows the FTIR spectrum of surface derivatization of dopamine with epichlorohydrin.

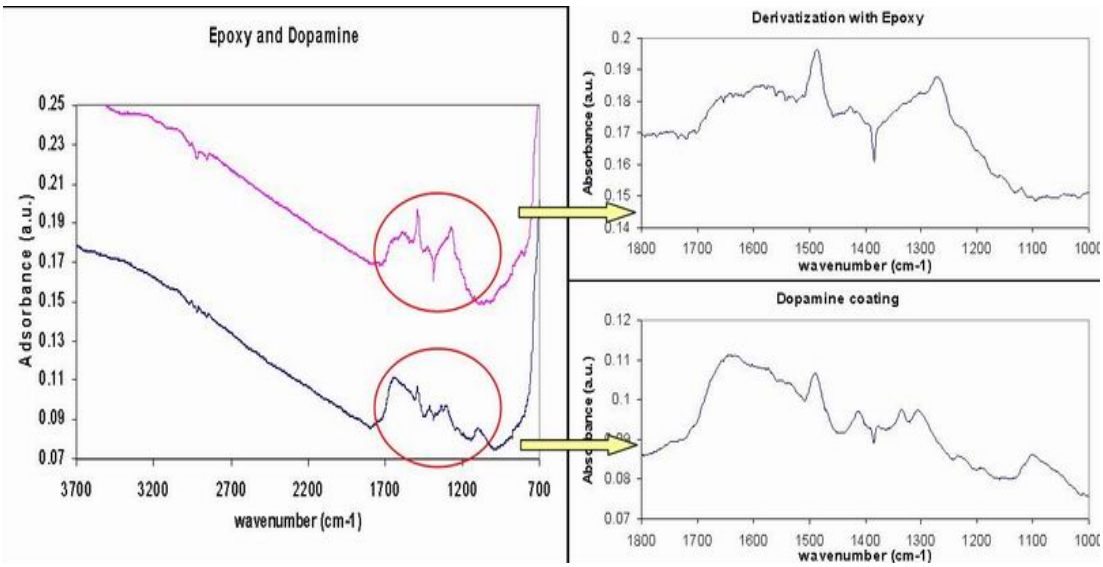

Figure 5-14: Comparison of FTIR spectra of epichlorohydrin functionalized surface with dopamine coating

Unfortunately, these spectra did not provide clear evidence of the presence of epoxy on the particle surface. Figure 5-12 shows the XPS spectra of dopamine coated nanoparticles with various additional coating. The C 1s high resolution analysis of the same sample showed only a slight increase in the component at 286 eV (due to the C-O bonds) which could result from epoxy groups. However, following the melting procedure of either mPEG-NH_2, as a control, or PEG-$(COOH)_2$, a large increase to C 1s at 286 eV was observed for PEG molecules (Figure 5-15). These results indicated the success of PEG grafting on epoxy derivatization of dopamine.

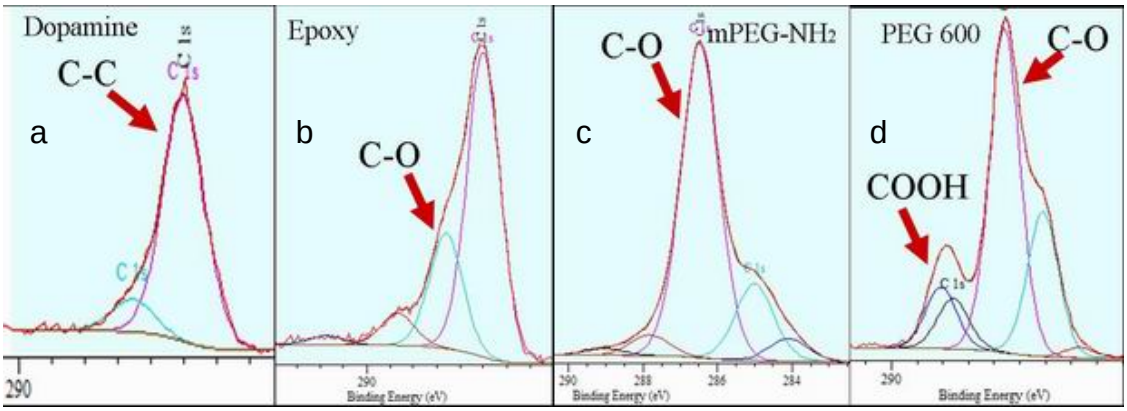

Figure 5-15: XPS C1s high resolution analyses spectra of dopamine coaing (a), derivative epoxy (b), mPEG-NH_2 coating on derivative epoxy (c) and PEG-$(COOH)_2$ (600) coating on derivative epoxy (d)

5.5.3 PEG-$(COOH)_2$ (600) versus PEG-$(COOH)_2$ (3,400)

The derivatization of dopamine and the melting strategy of PEG grafting provided the dopamine coated particles with a high density of PEG coating. However, the quality of nanoparticle suspension is still affected by the different molecular weight of the PEG. PEG-$(COOH)_2$ (600) and PEG-$(COOH)_2$ (3400) that have been grafted on the particles respectively, and compared for further understanding of the dynamic properties of PEG coating.

Figure 5-16: Stability of PEG (600) coating particles and PEG (3400) coating particles in MilliQ water

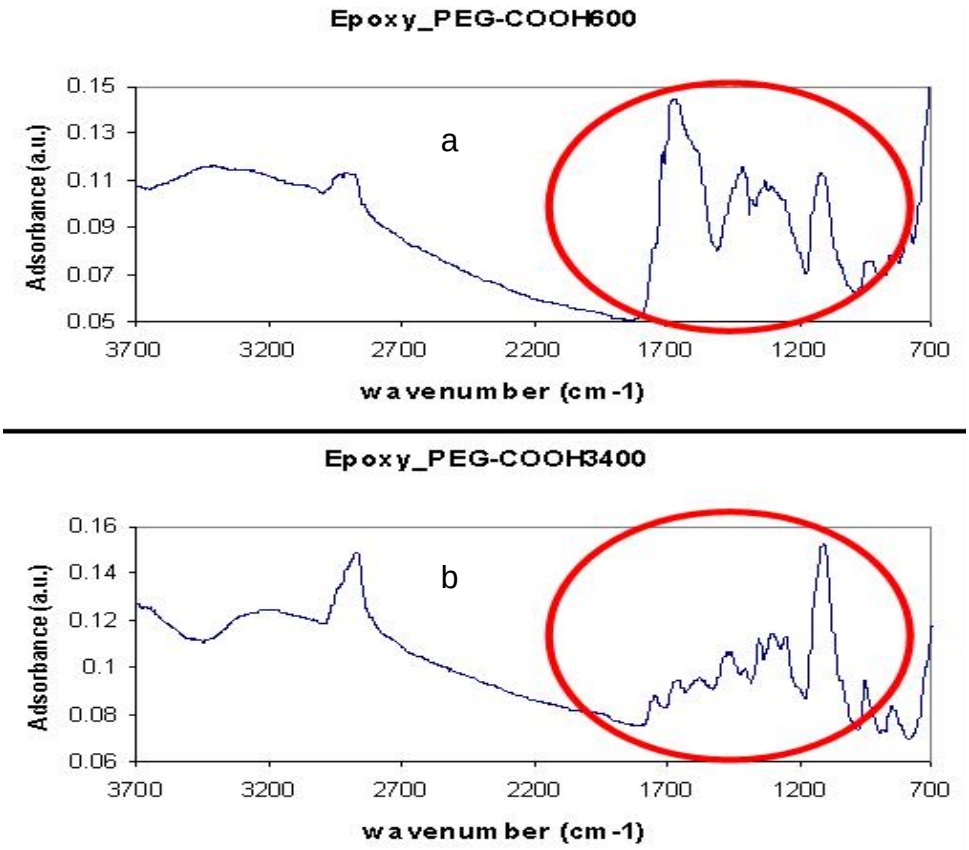

Figure 5-17: FTIR spectra of PEG (600) coating (a) and PEG (3400) coating (b) by melting strategy

As illustrated in Figure 5-16, the PEG (600) coating did not stabilize the particles, by contrast, the PEG (3400) coating stabilized the particles in MilliQ water extremely well. This could be due to the fact that PEG (600) has a much shorter and straighter molecular chain thus it would easily form crosslinkage between two nanoparticles, and then, forces the particles to agglomerate and form a bulk particle. Whereas that the PEG (3400) is longer chain molecule, the larger steric structure of the molecules reduced chance for the carboxyl groups on the other

end of the molecule to reach the new particles, so that the bent molecules prevented the particles from aggregation.

From the FTIR spectra shown in Figure 5-17, a large absorbance peak was observed on the PEG (600) coating spectrum at around 1750 cm^{-1} (attributed to -COOH groups) while there was only a small peak on PEG (3400) coating spectrum. This could be explained by lower density of carboxyl groups on PEG (3400) coating when the larger molecule of PEG (3400) had only two carboxyl groups attached to each end. On the other hand, both coatings experienced a sudden increase at from 1000 cm^{-1} to 1200 cm^{-1} (attributed to the PEG molecule chain). This signal was stronger on PEG (3400) coating. This could be attributed to higher density of PEG (600) on the particle surface than PEG (3400) because of its smaller molecular size. The PEG (3400) coating still provides a thicker polymer cover layer on the surface with its enormous molecular structure with fewer available carboxyl groups. Furthermore, the structure of PEG (3400) coating has advantage of resistance to non-specific protein adsorption without decreasing the stability of the particles in solvent caused by cross-linking on too many unoccupied –COOH groups. The TEM images displaying the structure of both PEG coatings strongly support the above conclusion (Figure 5-18).

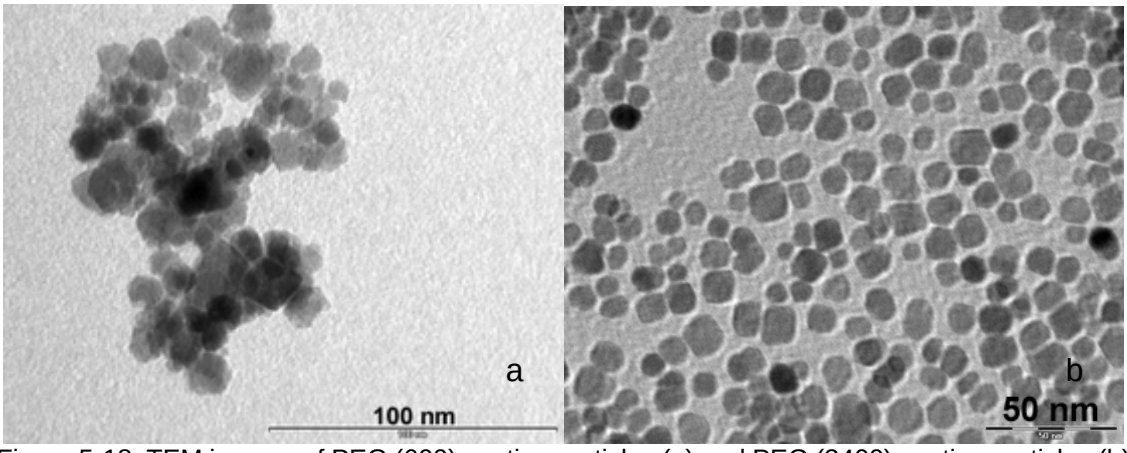

Figure 5-18: TEM images of PEG (600) coating particles (a) and PEG (3400) coating particles (b)

Figure 5-19: Stability of particles with dopamine coating (left), mPEG-NH_2 coating (middle) and PEG (3400) coating (right)

The high density of the PEG (3400) coating on the particle surface should theoretically provide un-reacted carboxyl groups for further functionalization. Figure 5-19 shows the stability of three different coating in PBS. Obviously, only the PEG (3400) coating could prevent aggregation and stabilized particles in PBS, because the un-reacted –COOH groups form negatively charged particle surfaces when PBS is used as the solvent. The repulsion between these nanoparticles was caused by identically charged surface with –COOH groups, and, thus, would not happen to the particles with the dopamine coating or the mPEG-NH_2 coating.

The high density and quality of PEG (3400) coating also influenced the stability of coated particles in various solvent. As shown in Figure 5-20, with the rising polarity of the solvents, the particles with PEG (3400) remained stable in CH_2Cl_2, $CHCl_3$, ethanol and H_2O. This performance clearly indicated the efficacy of the high density of PEG (3400) coating.

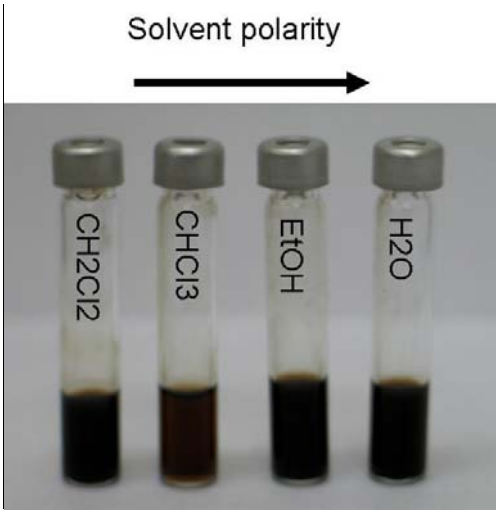

Figure 5-20: Stability of particles with PEG (3400) coating in various solvent. The solvent polarity increases from left to right.

5.6 Protein Adsorption

Along with colloidal stability in physiologically relevant conditions, another critical consideration in the surface modification of nanoparticles for *in vivo* applications is the resistance to non-specific adsorption of opsonin proteins. Opsonization initiates detection and phagocytosis of nanoparticles in the blood circulation, and results in sequestration in the organs of the mononuclear phagocytic system. Two oppositely charged proteins, negatively charged albumin and positively charged lysozyme, were tested on different coatings for the adsorption resistance of the non-specific protein.

A patented monoclonal antibody with molecular weight of approximately 17,000, provided by the Hanson Institute of The Royal Adelaide Hospital, was tested with both dextran and PEG coated particles as well as the corresponding antigen.

5.6.1 Dopamine Coating

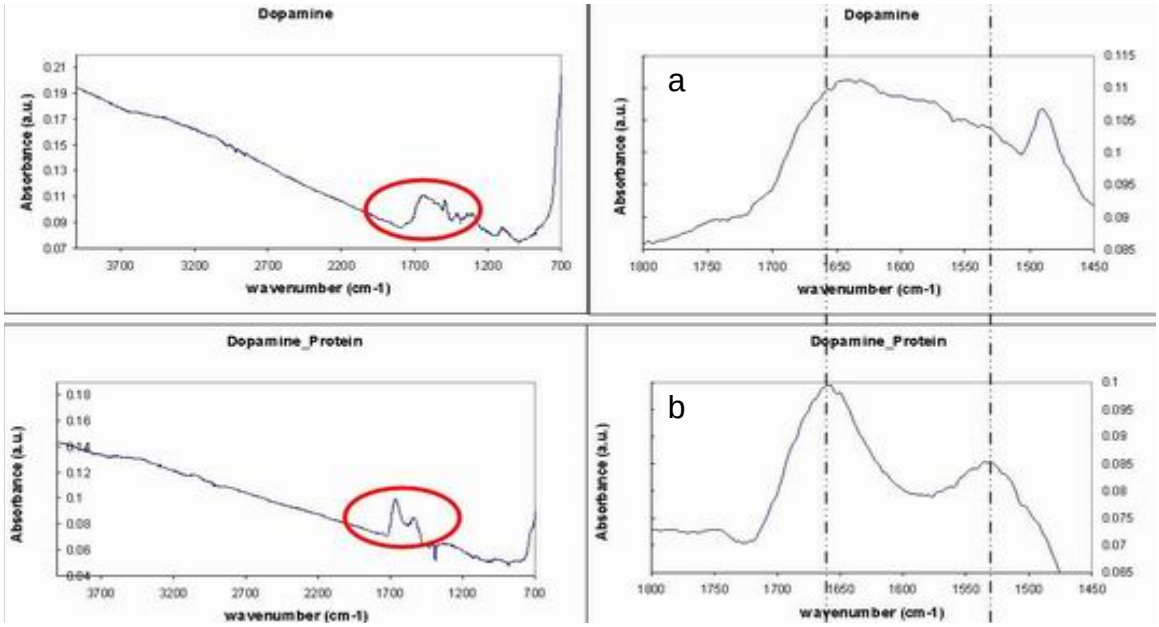

Figure 5-21: FTIR spectra of dopamine coating (a) and the protein adsorbed dopamine coating (b)

Dopamine coating has been examined where the amine groups stabilized particle suspension in H_2O. The FTIR spectra shown in Figure 5-21 clearly displays two significant rises of the characteristic amide I and II bands around

1550 cm^{-1} and 1650 cm^{-1} attributed to the two proteins. The dopamine has no ability to resist the adsorption of non-specific protein. This limits the bio-application of particles coated with dopamine and further functional molecule immobilization must be performed.

5.6.2 Dextran Coating

Previous studies have shown that dextran coatings can significantly reduce non-specific protein adsorption on the particle surface. The grafting procedure and resultant configuration of the macromolecules on the surface strongly influence the ability of these dextran coatings to resist non-specific adsorption of proteins.

Consequently, the *in vitro* investigation focused on the adsorption of two model proteins albumin and lysozyme on the dextran-coated nanoparticles. IR spectra for both dextran coating are displayed in Figure 5-22 to 5-23. The presence of proteins on the nanoparticles could be determined through the appearance of the characteristic amide I and II bands around 1650 cm^{-1} and 1550 cm^{-1}, respectively. Both dextran(1:2) and dextran(1:10) presented only small peaks at these wavelengths suggesting fairly low protein adsorption. By contrast, activated nanoparticles displayed a very strong protein signal, confirming the presence of the free carboxyl groups on the dextran-coated nanoparticles that could be activated to covalently immobilized biomolecules.

Similar results were obtained with a monoclonal antibody. Only three to five antibodies or antigens were expected to be attached to a single nanoparticle while the particles were mixed with an excess of five times the number of antibodies, so that XPS would be more sensitive in analysing chemical characteristics. The XPS survey spectra and C 1s high resolution analyses of antibody attached particles are shown in Figure 5-24 to 5-26.

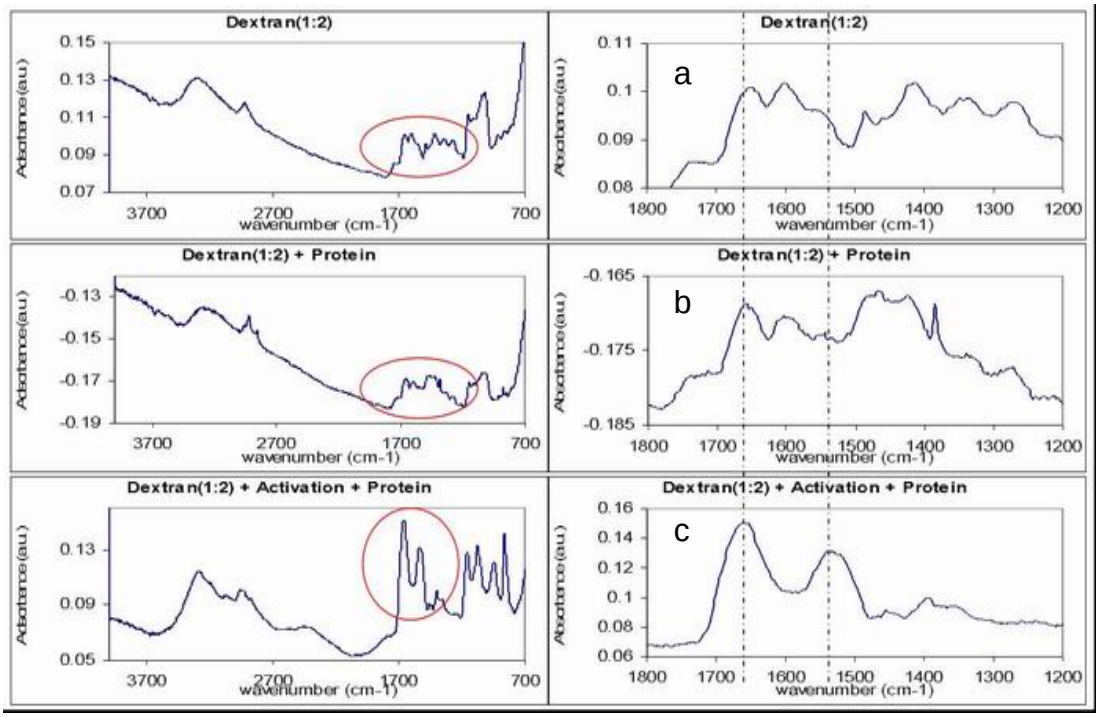

Figure 5-22: (a) IR spectrum of dextran(1:2) coated nanoparticles. (b) IR spectrum after protein adsorption. (c) IR spectrum after protein adsorption on activated nanoparticles. The dotted line shows the amide I and II bands associated with protein adsorption/immobilization.

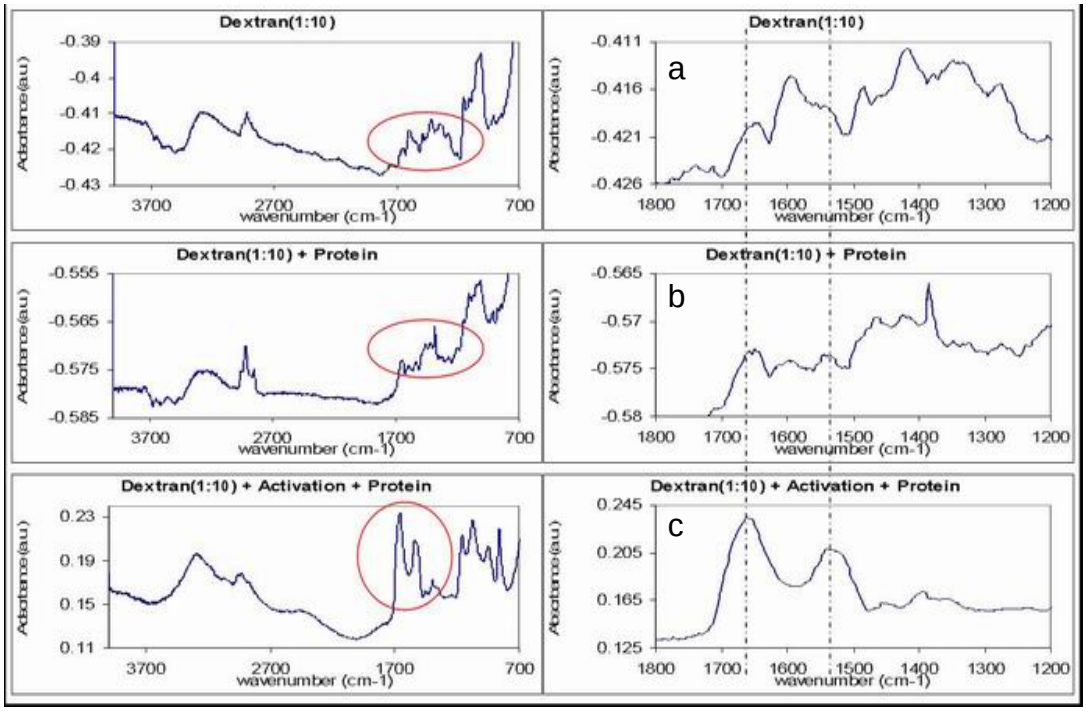

Figure 5-23: (a) IR spectrum of dextran(1:10) coated nanoparticles. (b) IR spectrum after protein adsorption. (c) IR spectrum after protein adsorption on activated nanoparticles. The dotted line shows the amide I and II bands associated with protein adsorption/immobilization.

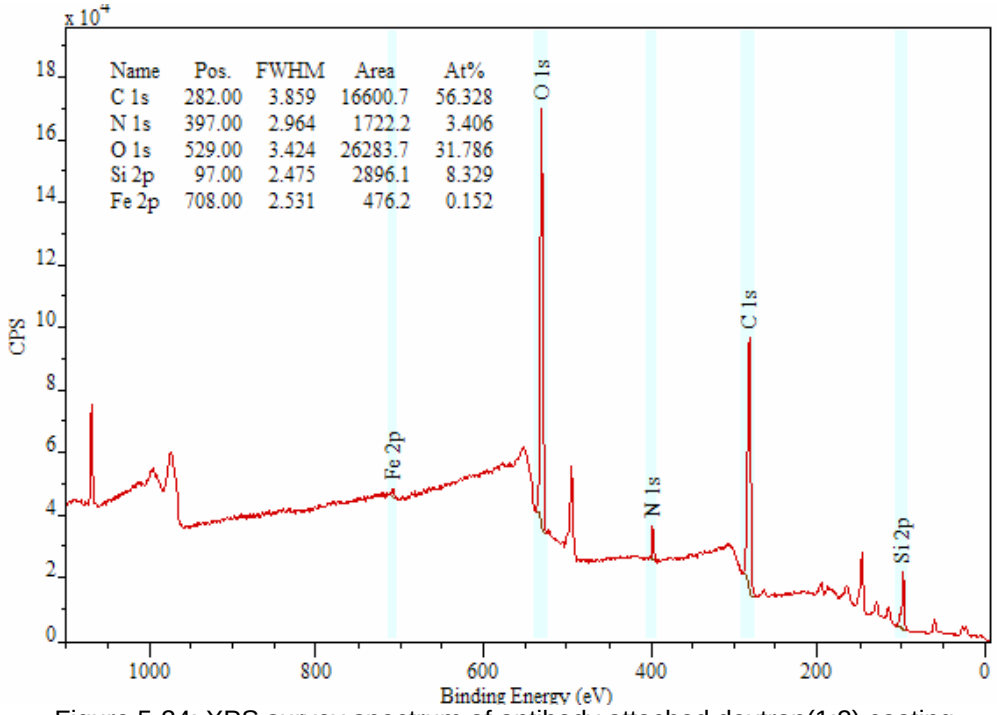

Figure 5-24: XPS survey spectrum of antibody attached dextran(1:2) coating

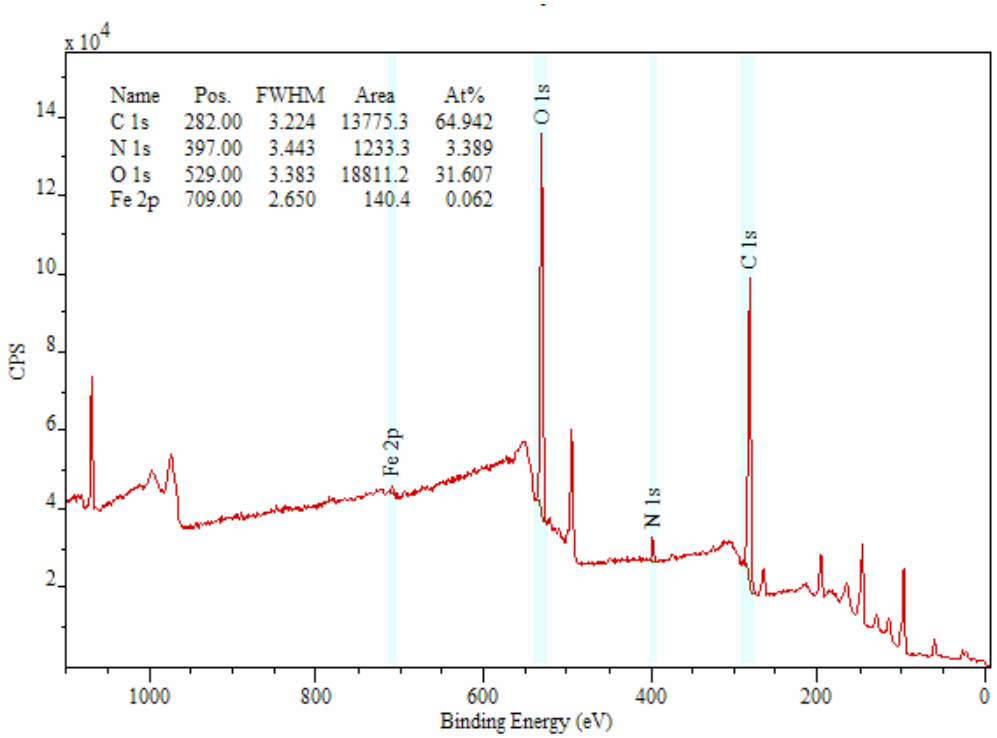

Figure 5-25: XPS survey spectrum of antibody attached dextran(1:10) coating

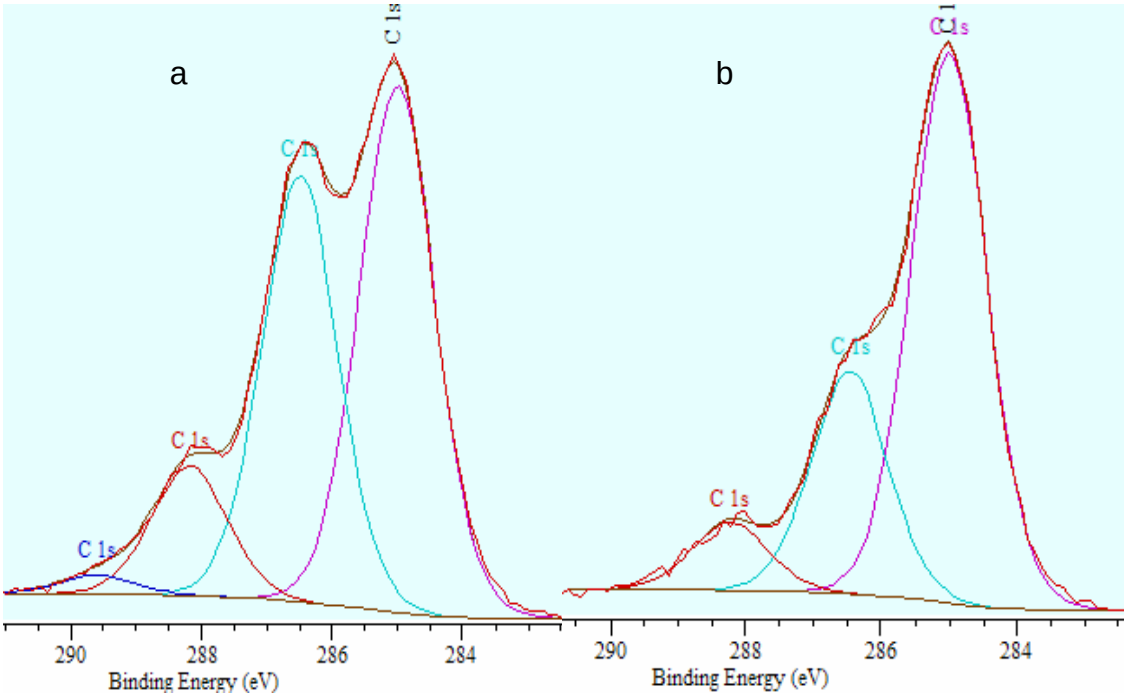

Figure 5-26: XPS C 1s high resolution analyses of antibody on dextran(1:2) (a) and on dextran(1:10) (b)

Compared to the C 1s high resolution analyses of dextran coating shown in the previous section (5.4), the evident increase at 285 eV of C1s indicates the presence of antibody. To confirm the success of antibody attachment, an *in vitro* test on cells is required. The bioactivity of the conjugated antibody is currently under investigation in the Hanson Institute. The ability to easily tune the reactivity of the carboxylmethyl dextran coated superparamagnetic particles is of high interest to researchers due to their potential use as immunotargeted MRI contrast agent.

5.6.3 PEG Coating

Similarly to the investigation on dextran coating, adsorption of two model proteins, albumin and lysozyme were also carried out on the PEG-coated nanoparticles. IR spectra for PEG (3400) coating are displayed in Figure 5-28, and mPEG-NH_2-coated particles were also examined as a control. It can be seen from these spectra that PEG (3400) presented only small peaks at wavelengths 1650 cm^{-1} and 1550 cm^{-1} thus suggesting fairly low protein adsorption. On the contrary, activated nanoparticles displayed a very strong protein signal, confirming the presence of free carboxyl group on the PEG

(3400)-coated nanoparticles that could be activated to covalently immobilized biomolecules. At the same time, the mPEG-NH_2 coating was found to adsorb a large amount of the two proteins (Figure 5-27). This can be concluded that PEG (3400) has a greater capability of resistance of non-specific adsorption of protein while it still provided un-reacted carboxyl groups for further functionalization.

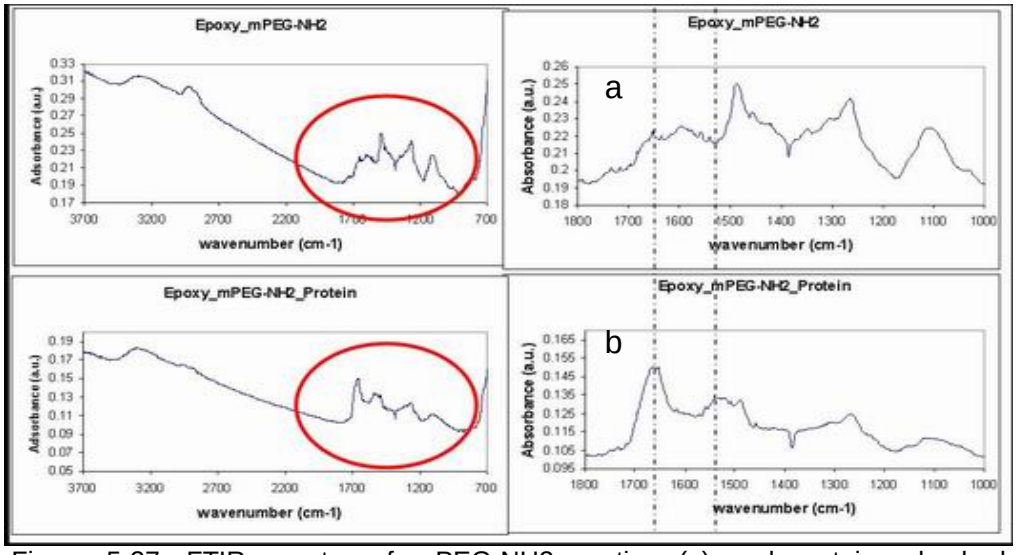

Figure 5-27: FTIR spectra of mPEG-NH2 coating (a) and protein adsorbed mPEG-NH2 coating (b)

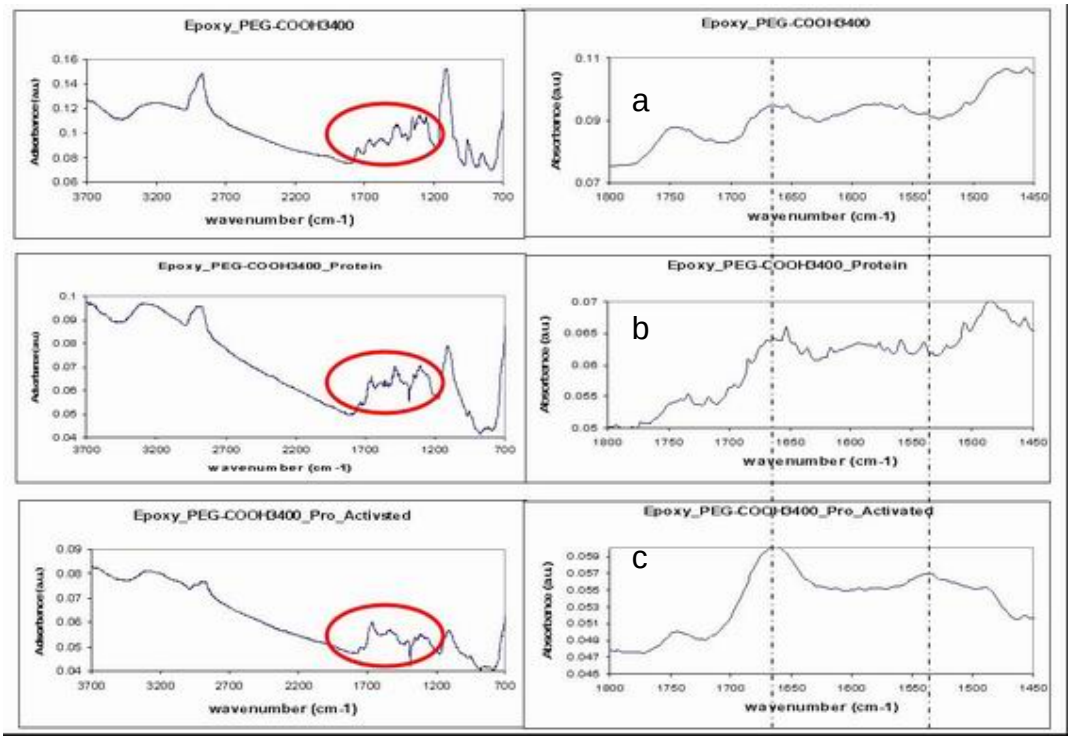

Figure 5-28: FTIR spectra of PEG (3400) coating (a), un-activating protein adsorbed PEG (3400) coating (b) and activating protein adsorbed PEG (3400) coating (c)

Due to the high density and quality of PEG (3400) coating, the magnetite nanoparticles are also under investigation with the patented monoclonal antibody provided by the Hanson Institute of the RAH. Preliminary *in vitro* experiments on cells gave positive results with these antibody attached PEG (3400)-coated particles. However, further work for confirming is still on going.

6 CONCLUSION

In this study, the co-precipitation technique and the non-aqueous route have been compared. Results from TEM show that both of the methods provided magnetite nanoparticles with a size distribution under 30 nm. However, aggregation has been observed in the samples where the co-precipitation technique was used. Because the co-precipitation method was generating the nanoparticles in an aqueous solvent, to control the quality of the particles, various parameters, such as pH, solvent concentration, reaction temperature and mix ratio of Fe^{3+} and Fe^{2+}, had to be adjusted appropriately and carefully. In addition, the generated particles needed to be stabilized immediately after synthesis to avoid agglomeration and sediment. In contrast, the non-aqueous route produced particles and prevents the particles from agglomeration with BA initially with ease, and hence the particles in BA could be kept much longer than those treated by co-precipitation technique without agglomeration.

Moreover, via the ligand exchange with the dopamine solution, the nanoparticles can be transferred to an aqueous dispersion phase easily. At the same time, the dopamine covalent bonding on particle surface with the hydroxyl groups stabilizes the particles in aqueous suspension and prevents them from the aggregation with a strong positively charged surface by these amine groups. In addition, the further surface modification with carboxymethylated dextran and carboxyl tailed PEG was successfully built up on the particle surface by reaction between carboxyl groups and amine groups provided by dopamine molecules.

The experiments have also shown that the quality of the immobilized functional molecule was affected by the structure of the surfactants. Less carboxymethyl containing dextran, dextran (1:10), has a better stability with almost no aggregation detected by DLS, as the dextran (1:2) coated particles have some small aggregation, as indicated by broadening of volume size distribution. In both cases of dextran coated particles, dextran coating slightly negatively charged the particle surface and formed perfect dispersion in aqueous solvent or in physiological brine. On the other hand, carboxyl PEG of the bigger molecule,

PEG (3400), protected aggregation of particles more significantly than of smaller one, PEG (600). More impressively, the PEG (3400) coated particles show a great stability in various solvents.

No or minimal adsorption of the non-specific protein has been observed on both dextran coating and PEG coating with un-activated carboxyl groups. However, activated carboxyl groups could bond with mixture of albumin and lysozyme; this indicated that the activity of remaining carboxyl groups after grafting of dextran or PEG could be controlled.

The particles with dextran coating or PEG coating have been attached by the monoclonal antibodies or antigens as control, for further study in the Hanson Institute of RAH. This study is continuing.

The present study has created dextran coating and PEG coating on magnetite nanoparticles by the non-aqueous route in aqueous suspension for MRI application as well as for other *in vivo* applications. The stability of the dispersion, the capability of non-specific protein adsorption resistance and availability of un-reacted carboxyl groups on the particle surface offers these particles a potential for various bio-applications, although further *in vitro* experiments have to be done before these applications can be considered.

APPENDIX A

XPS survey and C 1s high-resolution spectra of pure PEG (600) and PEG (3400)

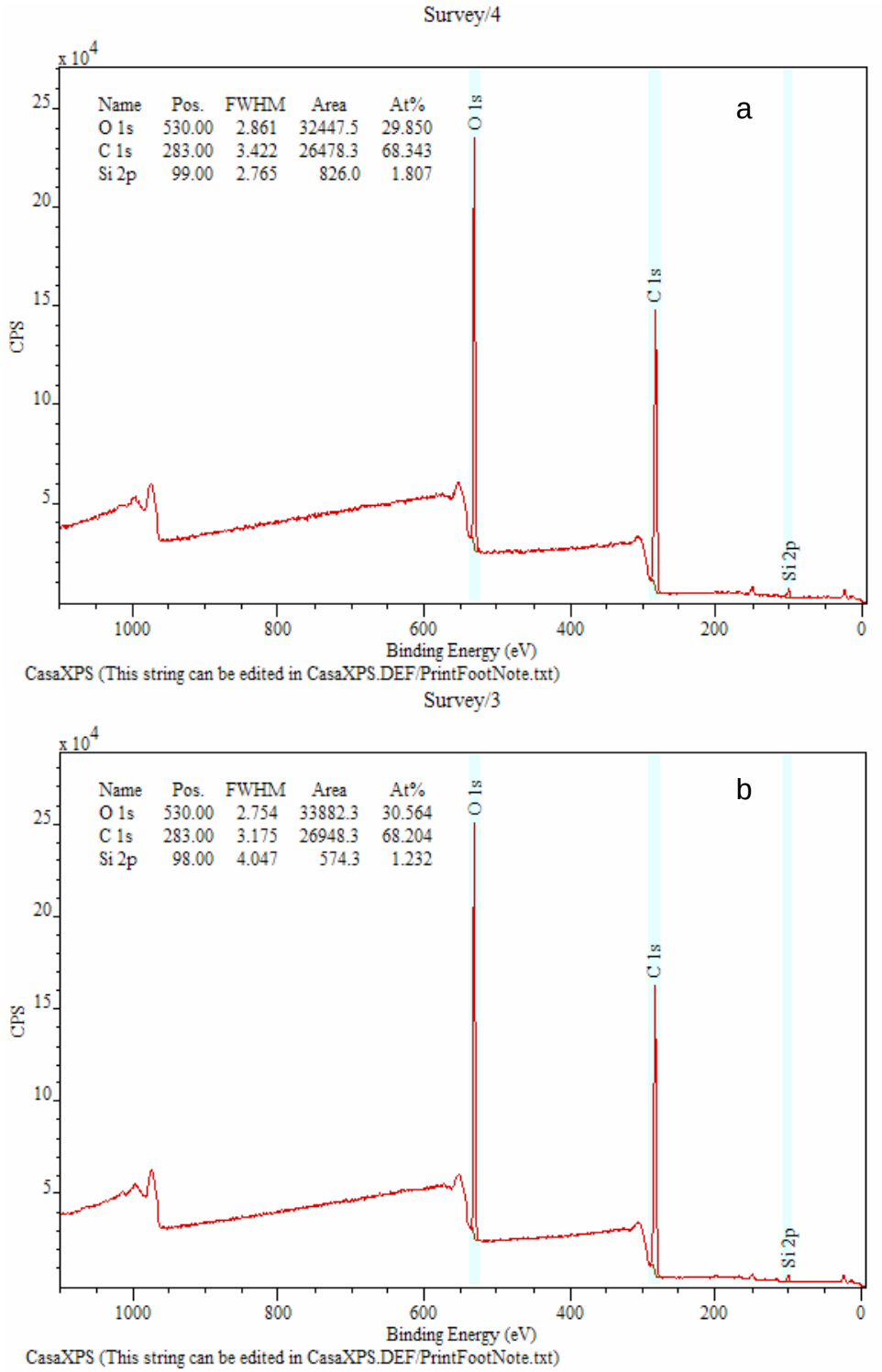

Figure i: XPS survey spectra of PEG (600) (a) and PEG (3400) (b)

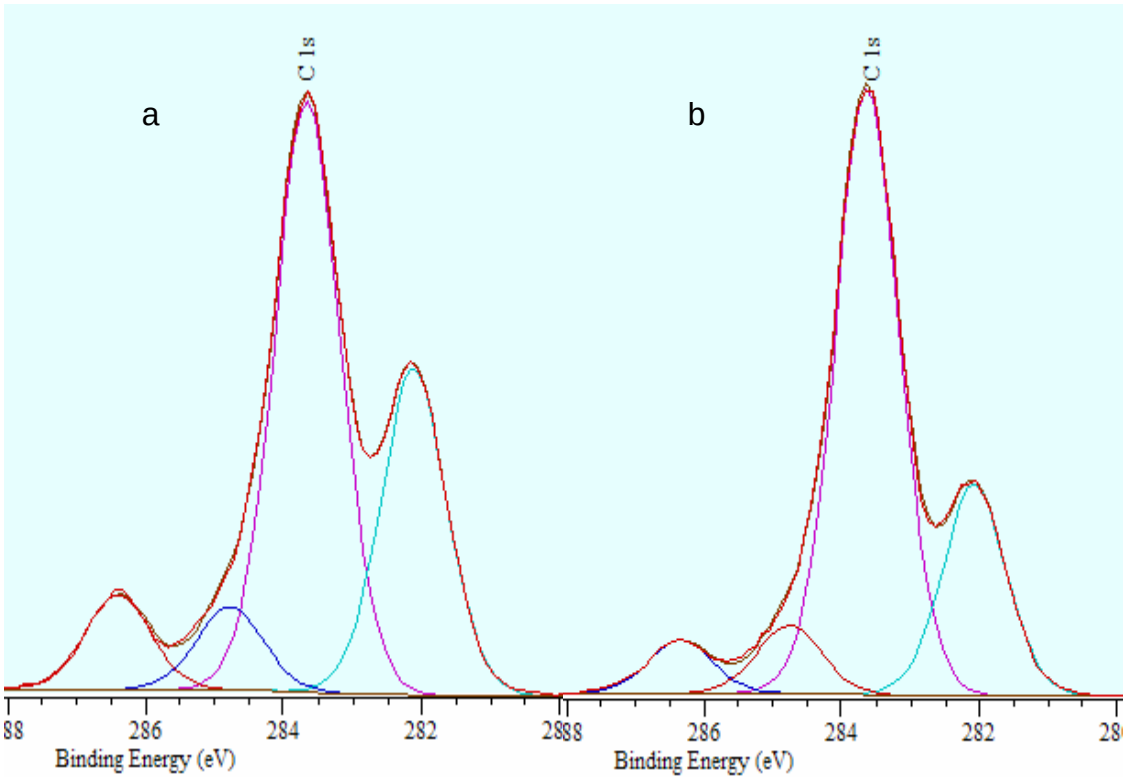

Figure ii: C 1s high-resolution spectra of PEG (600) (a) and PEG (3400) (b)

APPENDIX B

Results of relevant study on gold particles (by B. Thierry)

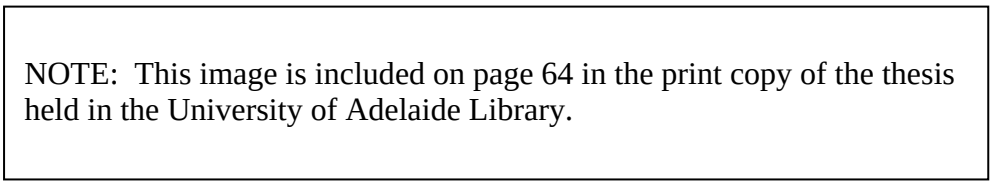

Figure iii: TEM image of dextran coated fold nanoparticles

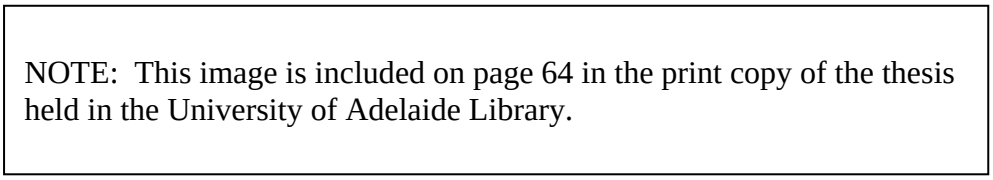

Figure iv: DLS size distribution by volume of gold nanoparticles with different coatings

NOTE: These images are included on page 65 of the print copy of the thesis held in the University of Adelaide Library.

Figure v: Photographs of suspension of gold nanoparticles with dex (1:10) coating (a) and dex (1:2) (b)

REFERENCES

Abu Mukh-Qasem, R. and Gedanken, A. (2005). *Sonochemical synthesis of stable hydrosol of Fe_3O_4 nanoparticles*. Journal of Colloid and Interface Science **284**(2): 489-494.

Alexiou, C., Arnold, W., et al. (2000). *Locoregional cancer treatment with magnetic drug targeting*. Cancer Research **60**(23): pp 6641-6648.

Bautista, M. C., Bomati-Miguel, O., et al. (2005). *Surface Characterisation of Dextran-coated Iron Oxide Nanoparticles Prepared by Laser Pyrolysis and Coprecipitation*. JOURNAL OF MAGNETISM AND MAGNETIC MATERIALS **293**(2005): 20-27.

Bee, A., Massart, R., et al. (1995). *Synthesis of very fine maghemite particles*. Journal of Magnetism and Magnetic Materials **149**: pp 6-9.

Bharali, D. J., Sahoo, S. K., et al. (2003). *Cross-linked polyvinylpyrrolidone nanoparticles: A potential carrier for hydrophilic drugs*. Journal of Colloid and Interface Science **258**(2): pp 415-423.

Bordat, C., Sich, M., et al. (2000). *Distribution of iron oxide nanoparticles in rat lymph nodes studied using electron energy loss spectroscopy (EELS) and electron spectroscopic imaging (ESI)*. Journal of magnetic resonance imaging **12**(3): pp 505-509.

Burke, N. A. D., Stover, H. D. H., et al. (2001). *Preparation and Characterization of Polymer-Coated Magnetic Nanoparticles*. IEEE **37**(4).

Chambon, C., Clement, O., et al. (1993). *Superparamagnetic iron oxides as positive MR contrast agents: in vitro and in vivo evidence*. Journal of Magnetic resonance imaging **11**(4): pp 509-519.

Chouly, C., Pouliquen, D., et al. (1996). *Development of superparamagnetic nanoparticles for MRI: effect of particle size, charge and surface nature on biodistribution*. Journal of Microencapsulation **13**(3): pp 245-255.

Feeney, J. (1996). *Magnetic Resonance Imaging -- A Window into the Human Body*. **2004**.

Frahm, J., Dechent, P., et al. (2003). *Advances in functional MRI of the human brain*. Progress in Nuclear Magnetic Resonance Spectroscopy **44**(2004): pp

1-32.

Frenkel, J. and Dorfman, J. (1930). *Spontaneous and induced magnetisation in ferromagnetic bodies*. Nature **126**: pp 274-275.

Gangopadhyay, P., Gallet, S., et al. (2005). *Novel superparamagnetic core(shell) nanoparticles for magnetic targeted drug delivery and hyperthermia treatment*. IEEE Transactions on Magnetics **41**(10): 4194-4196.

Gao, Y. (2003). *Use of water-dispersible Fe_2O_3 nanoparticles with narrow size distributions in isolating avidin*. Journal of Colloid and Interface Science **266**: pp 215-218.

Gee, S. H., Hong, Y. K., et al. (2003). *Synthesis and aging effect of spherical magnetite (Fe_3O_4) nanoparticles for biosensor applications*. Journal of Applied Physics **93**(10 2): 7560-7562.

Gonzales, M. and Krishnan, K. M. (2005). *Synthesis of magnetoliposomes with monodisperse iron oxide nanocrystal cores for hyperthermia*. Journal of Magnetism and Magnetic Materials **293**(1): 265-270.

Gref, R., Domb, A., et al. (1995). *The controlled intravenous delivery of drugs using PEG-coated sterically stabilized nanospheres*. Advanced Drug Delivery Review **16**(2,3): pp 215-233.

Griesser, H. J., Hartley, P. G., et al. (2002). *Interfacial Properties and Protein Resistance of Nano-scale Polysaccharide Coating*. Smart Materials and Structures **11**(2002): 652-661.

Gupta, A. K. and Gupta, M. (2004). *Synthesis and Surface Engineering of Iron Oxide Nanoparticles for Biomedical Applications*. Biomaterials(26): pp 3995-4021.

Harisinghani, M. G., Barentsz, J., et al. (2003). *Noninvasive Detection of Clinically Occult Lymph-Node Metastases in Prostate Cancer*. The New England Journal of Medicine **348**(25): pp 2491-2499.

Harris, L. A., Goff, J. D., et al. (2003). *Magnetite Nanoparticle Dispersions Stabilized with Triblock Copolymers*. Chemical Materials.

Hartley, P. G., McArthur, S. L., et al. (2001). *Physicochemical Properties of Polysaccharide Coatings Based on Grafted Multilayer Assemblies*. International Journal of Pharmaceutics **18**(2002): 2483-2494.

Hasegawa, M., Ito, Y., et al. (1998). *Water-soluble carboxypolysaccharide - magnetic iron oxide complex having a small particle diameter*. USA, MEITO SANGYO KABUSHIKI KAISHA

Hong, R., Fischer, N. O., et al. (2005). *Surface PEGylation and Ligand Exchange Chemistry of FePt Nanoparticles for Biological Application*. International Journal of Pharmaceutics **17**(2005): 4617-4621.

Horn, D. and Rieger, J. (2001). *Organic nanoparticles in the aqueous phase - Theory, experiment, and use*. Angewandte Chemie - International Edition **40**(23): pp 4330-4361.

Hyeon, T., Su Seong, L., et al. (2001). *Synthesis of highly crystalline and monodisperse maghemite nanocrystallites without a size-selection process*. Journal of the American Chemical Society **123**(51): 12798-12801.

Illum, L., Davis, S. S., et al. (1987). *The organ distribution and circulation time of intravenously injected colloidal carriers sterically stabilized with a block copolymer-poloxamine 908*. Life Sciences **40**(4): pp 367-374.

Ito, A., Kuga, Y., et al. (2004). *Magnetite Nanoparticle-Loaded Anti-Her2 Immunoliposomes for Combination of Antibody Therapy with Hyperthermia*. Cancer Letters **212**: pp 167-175.

Ivkov, R., Denardo, S. J., et al. (2005). *Application of High Amplitude Alternating Magnetic Fields for Heat Induction of Nanoparticles Localized in Cancer*. Clinical Cancer Research **11**: pp 7093S-7103S.

Jordan, A., Scholz, R., et al. (1999). *Magnetic fluid hyperthermia (MFH): cancer treatment with AC magnetic field induced excitation of biocompatible superparamagnetic nanoparticles*. Journal of Magnetism and Magnetic Materials **201**: pp 413-419.

Jun, Y. W., Huh, Y. M., et al. (2005). *Nanoscale Size Effect of Magnetic Nanocrystals and Their Utilization for Cancer Diagnosis Via Magnetic Resonance Imaging*. Journal of the American Chemical Society **127**: pp 5732-5733.

Kim, D. K., Toprak, M., et al. (2002). *Surface Modification of Superparamagnetic Nanoparticles for in-vivo Biomedical Applications*. Nanoparticulate Materials, Nov 26-29 2001, Boston, MA, United States, Materials Research Society.

Kim, J.-Y., Shin, D.-H., et al. (2004). *Synthesis of nanophase-separated poly(urethane-co-acrylic acid) network films and their application for magnetic nanoparticle synthesis*. Journal of Applied Polymer Science **91**(6): 3549-3556.

Kingshott, P., Thissen, H., et al. (2002). *Effects of cloud-point grafting , chain length, and density of PEG layers on competitive absorption of ocular proteins*. Biomaterials **23**: pp 2043-2056.

Kreuter, J. (1983). *Evaluation of nanoparticles as drug-delivery systems I: preparation methods*. Pharmaceutica Acta Helvetiae **58**(7): pp 196-209.

Lacava, Z. G. M., Azevedo, R. B., et al. (1999[1]). *Toxic effects of ionic magnetic fluids in mice*. Journal of Magnetism and Magnetic Materials **194**(1-3): pp 90-95.

Lacava, Z. G. M., Azevedo, R. B., et al. (1999[2]). *Biological effects of magnetic fluids: toxicity studies*. Journal of Magnetism and Magnetic Materials **201**: pp 431-434.

Lee, H. S., Kim, E. H., et al. (2005). *Synthesis of SPIO-chitosan microspheres for MRI-detectable embolotherapy*. Journal of Magnetism and Magnetic Materials **293**: pp 102-105.

Liz-Marzan, L. M. (2004). *Nanoparticles: formation and color*. Materialstoday. **Februrary:** pp 26-31.

Lubbe, A. S. and Bergemann, C. (1996). *Selected preclinical and first clinical experiences with magnetically targeted 4'-epidoxorubicin inpatients with advanced solid tumors*. Scientific and Clinical Applications of Magnetic Carriers, Rostock, Germany, Plenum, New York.

Lubbe, A. S., Bergemann, C., et al. (1999). *Physiological aspects in magnetic drug-targeting*. Journal of Magnetism and Magnetic Materials **194**(1-3): pp 149-155.

Lubbe, A. S., Bergemann, C., et al. (1996). *Clinical experiences with magnetic drug targeting: a phase I study with 4'-epidoxorubicin in 14 patients with advanced solid tumors*. Cancer research **56**(20): pp 4686-4693.

Mclean, K. M., Johnson, G., et al. (2000). *Method of immobilization of carboxymethyl-dextran affects resistance to tissue and cell colonization*. Colloids Surf B Biointerfaces **18**: pp 221-234.

Meza, M. (1996). *Application of magnetic particles in immunoassays*. Scientific and Clinical Applications of Magnetic Carriers, Rostock, Germany, Plenum, New York.

Moghimi, S. M., Hedeman, H., et al. (1993). *An investigation of the filtration capacity and the fate of large filtered sterically-stabilized microspheres in rat spleen*. Biochimica et Biophysica Acta **1157**(3): pp 233-240.

Muller, R. H., Luck, M., et al. (1996). *Intravenously injected particles: surface properties and interaction with blood proteins-the key determining the organ distribution*. Scientific and Clinical Applications of Magnetic Carriers, Rostock, Germany, Plenum, New York.

Neuberger, T., Schopf, B., et al. (2005). *Superparamagnetic nanoparticles for biomedical applications: Possibilities and limitations of a new drug delivery system*. Journal of Magnetiam and Magnetic Materials **293**: pp 483-496.

Nitin, N., LaConte, L. E. W., et al. (2004). *Functionalization and peptide-based delivery of magnetic nanoparticles as an intracellular MRI contrast agent*. J Biol Inorg Chem **9**: pp 706-712.

Olsvik, O., Popovic, T., et al. (1994). *Magnetic separation techniques in diagnostic microbiology*. Clinical microbiology reviews **7**(1): pp 43-54.

Oppenheim, R. C. (1981). *Solid colloidal drug delivery systems: nanoparticles*. International Journal of Pharmaceutics **8**(3): pp 217-234.

Owens III, D. E. and Peppas, N. A. (2005). *Opsonization, Biodistribution, and Pharmacokinetics of Polymeric Nanoparticles*. International Journal of Pharmaceutics **307**(2006): 93-102.

Panagi, Z., Beletsi, A., et al. (2001). *Effect of dose on the biodistribution and pharmacokinetics of PLGA and PLGA-mPEG nanoparticles*. International Journal of Pharmaceutics **221**(1-2): pp 143-152.

Pasche, S., Textor, M., et al. (2005[1]). *Relationship Between Interfacial Forces Measured by Colloid-Probe Atomic Force Microscopy and Protein Resistance of Poly(ethylene glycol)-Grafted Poly(L-Lysine) Adlayers on Niobia Surfaces*. Langmuir **21**: pp 6508 6520.

Pasche, S., Voros, J., et al. (2005[2]). *Effects of Ionic Strength and Surface Charge on Protein Absorption at PEGylated Surface*. Journal of Physical Chemistry B **109**: pp 17545-17552.

Pinna, N., Grancharov, S., et al. (2005). *Magnetite Nanocrystals: Nonaqueous Synthesis, Characterization, and Solubility*. Journal of the American Chemical Society **17**: 3044-3049.

Portet, D., Denizot, B., et al. (2001). *Nonpolymeric Coatings of Iron Oxide Colloids for Biological Use as Magnetic Resonance Imaging Contrast Agents*. Journal of Colloid and Interface Science **238**(1): pp 37-42.

Poste, G., Kirsh, R., et al. (1984). *The challenge of liposome targeting in vivo*. Liposome Technology, PA, USA, CRC, Boca Raton, Fla.

Prestvik, W. S., Berge, A., et al. (1996). *Preparation and application of monosized magnetic particles in selective cell separation*. Scientific and Clinical Applications of Magnetic Carriers, Rostock, Germany, Plenum, New York.

Puntes, V. F., Krishnan, K. M., et al. (2001). *Colloidal Nanocrystal Shape and Size Control: The Case of Cobalt*. Science **291**: pp 2115-2117.

Santra, S., Tapec, R., et al. (2001). *Synthesis and Characterization of Silica-Coated Iron Oxide Nanoparticles in Microemulsion: The Effect of Nonionic*

Surfactants. Langmuir **17**(10): pp 2900-2906.

Schmidt, H. (2001). *Nanoparticles by chemical synthsis, processing to materials and innovative applications*. Appl. Organometal. Chem.(15): pp 331-343.

Schutt, W., Gruttner, C., et al. (1997). *Applications of magnetic targeting in diagnosis and therapy--possibilities and limitations: a mini-review*. Hybridoma **16**(1): pp 109-117.

Schutt, W., Gruttner, C., et al. (1999). *Biocompatible magnetic polymer carriers for in vivo radionuclide delivery*. Artificial Organs **23**(1): pp 98-103.

Song, H.-T., Choi, J.-s., et al. (2005). *Surface Modulation of Magnetic Nanocrystals in the Development of Highly Efficient Magnetic Resonance Probes for Intracellular Labeling*. Journal of the American Chemical Society

Sun, S. (2004). *Monodisperse MFe_2O_4 (M=Fe, Co, Mn) Nanoparticles*. Journal of the American Chemical Society **126**: pp 273-279.

Sun, S. H. (2006). *Recent Advances in Chemical Synthesis, Self-Assembly, and Applications of Fept Nanoparticles*. Advanced Materials **18**: pp 393-403.

Tartaj, P., Morales, M. P., et al. (2005). *Advances in Magnetic Nanoparticles for Biotechnology Applications*. Journal of Magnetiam and Magnetic Materials **290**: pp 28-34.

Torchilin, V. P. (2000). *Drug targeting*. European Journal of Pharmaceutical Sciences **11**(Suppl.2): pp S81-S91.

Weissleder, R., Stark, D. D., et al. (1989). *Superparamagnetic iron oxide: pharmacokinetics and toxicity*. American Journal of roentgenology **152**(1): pp 167-173.

Xu, C., Xu, K., et al. (2004). *Dopamine as A Robust Anchor to Immobilize Functional Molecules on the Iron Oxide Shell of Magnetic Nanoparticles*. Journal of the American Chemical Society **126**: 9938-9939.

Zhang, Y. and Zhang, J. (2005). *Surface Modification of Monodisperse Magnetite Nanoparticles for Improved Intracellular Uptake to Breast Cancer Cells*. Journal of Colloid and Interface Science **283**: 352-357.